Advances in Water Resources 91 (2016) 46–62

Contents lists available at ScienceDirect

Advances in Water Resources

journal homepage: www.elsevier.com/locate/advwatres

Mechanisms of shrub encroachment into Northern Chihuahuan Desert grasslands and impacts of climate change investigated using a cellular automata model

Domenico Caracciolo[a,*], Erkan Istanbulluoglu[b], Leonardo Valerio Noto[c], Scott L. Collins[d]

[a] Dipartimento di Ingegneria Civile, Ambientale, Aerospaziale, dei Materiali (DICAM), Università degli Studi di Palermo, Palermo, Italy
[b] Department of Civil and Environmental Engineering, University of Washington, Seattle, WA 98195, USA
[c] Dipartimento di Ingegneria Civile, Ambientale, Aerospaziale, dei Materiali (DICAM), Università degli Studi di Palermo, Palermo, Italy
[d] Department of Biology, University of New Mexico, Albuquerque, NM 87131-0001, USA

ARTICLE INFO

Article history:
Received 27 January 2015
Revised 12 February 2016
Accepted 3 March 2016
Available online 10 March 2016

Keywords:
Shrub encroachment
Climate change
CA model
Ecohydrology

ABSTRACT

Arid and semiarid grasslands of southwestern North America have changed dramatically over the last 150 years as a result of woody plant encroachment. Overgrazing, reduced fire frequency, and climate change are known drivers of woody plant encroachment into grasslands. In this study, relatively simple algorithms for encroachment factors (i.e., grazing, grassland fires, and seed dispersal by grazers) are proposed and implemented in the ecohydrological Cellular-Automata Tree Grass Shrub Simulator (CATGraSS). CATGraSS is used in a 7.3 km^2 rectangular domain located in central New Mexico along a zone of grassland to shrubland transition, where shrub encroachment is currently active. CATGraSS is calibrated and used to investigate the relative contributions of grazing, fire frequency, seed dispersal by herbivores and climate change on shrub abundance over a 150-year period of historical shrub encroachment. The impact of future climate change is examined using a model output that realistically represents current vegetation cover as initial condition, in a series of stochastic CATGraSS future climate simulations. Model simulations are found to be highly sensitive to the initial distribution of shrub cover. Encroachment factors more actively lead to shrub propagation within the domain when the model starts with randomly distributed individual shrubs. However, when shrubs are naturally evolved into clusters, the model response to encroachment factors is muted unless the effect of seed dispersal by herbivores is amplified. The relative contribution of different drivers on modeled shrub encroachment varied based on the initial shrub cover condition used in the model. When historical weather data is used, CATGraSS predicted loss of shrub and grass cover during the 1950 s drought. While future climate change is found to amplify shrub encroachment (~13% more shrub cover by 2100), grazing remains the dominant factor promoting shrub encroachment. When we modeled future climate change, however, encroachment still occurred at a reduced rate in the absence of grazing along with pre-grazing fire frequency because of lower shrub water stress leading to reduced shrub mortality which increases the probability of shrub establishment.

1. Introduction

Arid and semiarid grasslands of southwestern North America have changed dramatically over the last ~150 years as a result of woody plant encroachment (WPE) [5,16,19,47,85,93]. WPE is defined as an increase in the density, cover, and biomass of native trees or shrubs in grasslands [9,19,33,34,55]. Encroachment of native woody species has greatly changed the appearance and structure of many former semiarid grasslands to shrublands, brushlands, or woodlands [55]. Repeat photography clearly illustrates encroachment of juniper trees into grasslands west of Albuquerque, New Mexico, US (Fig. 1a and b) [3], and shrub encroachment into grasslands in southeastern Arizona, US (Fig. 1c, d and e) [9].

Recent studies have summarized the positive and negative impacts of WPE into neighboring plant communities during the past 150 years (e.g., [36,75]), however in many areas, such as the Southwestern US and Southern Africa, rapid expansion by shrubs has caused considerable concern because of increased soil erosion, reduced stream flows, altered wildlife habitat, reduced forage production, and changes in plant community composition and diversity [7,77,90–92].

* Corresponding author. Tel.: +3909123896544.
E-mail addresses: domenico.caracciolo@unipa.it (D. Caracciolo), erkani@u.washington.edu (E. Istanbulluoglu), leonardo.noto@unipa.it (L.V. Noto), scollins@sevilleta.unm.edu (S.L. Collins).

http://dx.doi.org/10.1016/j.advwatres.2016.03.002
0309-1708/

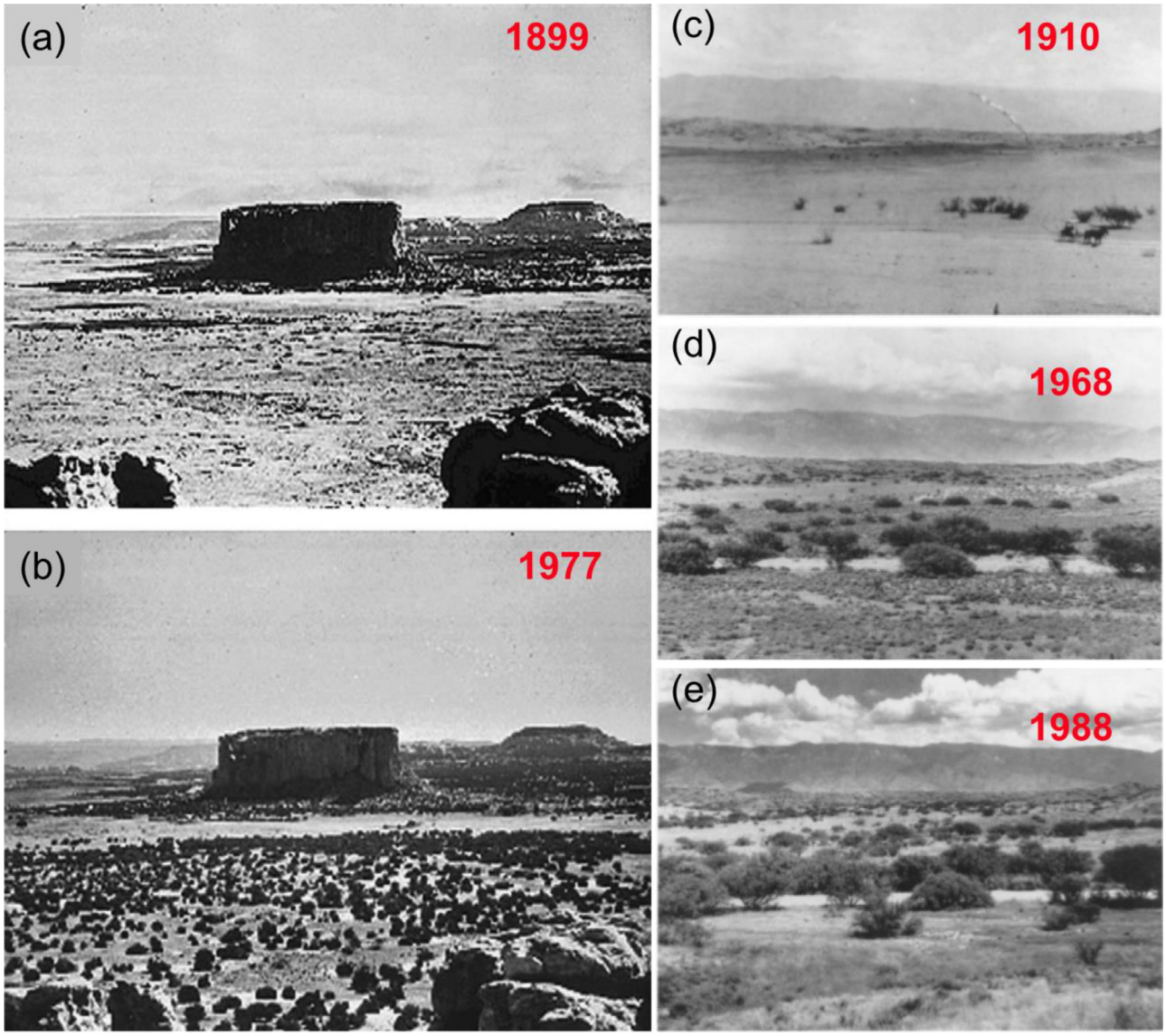

Fig. 1. Illustration of woody plant encroachment using repeat photography: juniper trees encroach into grasslands west of Albuquerque, New Mexico, USA. Photographs show Enchanted Mesa taken from Acoma Pueblo in (a) 1899 taken by W.H. Jackson, used with permission from the History Colorado, the Colorado Historical Society, and (b) 1977 taken by H.E. Malde, used with permission from the U.S. Geological Survey (from http://cpluhna.nau.edu/Research/grasslands1.htm, [3]). Shrub encroachment in grasslands in southeastern Arizona, USA: (c) 1910, photograph by O.E. Meinzer, courtesy of the U.S. Geological Survey, used with permission from Wiley library, (d) 1968, photograph by R.M. Turner, courtesy of the U.S. Geological Survey, used with permission from Wiley library, (e) 1988, photograph by C.J. Bahre (from [9]), used with permission from Wiley library.

Although some earlier studies have related WPE in semiarid grasslands to a single dominant factor, such as fire or grazing (e.g., [10,17,18,21]), growing evidence points to the interaction of several cascading factors driven by the introduction of domestic herbivores in the southwest US (e.g., Fig. 2; [34,63,92,93]). Essentially, loss of grass biomass and fine fuels through chronic high levels of grazing in this region have resulted in a significant reduction in grassland fire frequency from an approximate historic return period of 10 years to 100 years since the beginning of grazing [5,21,79,92]. Grassland fires suppress the growth and encroachment of trees and shrubs [31,44,93,97] and increase splash, runoff and aeolian erosion, with a subsequent homogenizing effect on spatial distribution of resources that may favor healthy grass regrowth [35,78,95]. With less frequent and more intense fires, woody plant mortality decreases as shown by several fire control experiments, and maturing woody plants produce seeds for dispersal to surrounding bare soil patches (e.g., [13,77,83]). In addition, deposition of resources eroded from burned and grazed patches promotes the formation of shrub patches, known as “islands of fertility” [26,79,85].

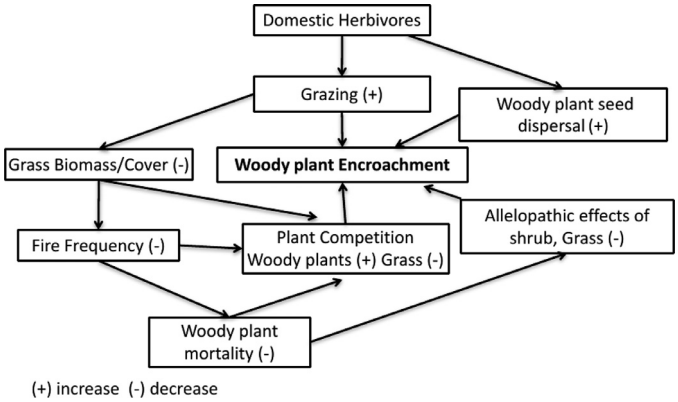

Fig. 2. Conceptual model illustrating interactions of processes associated with woody plant encroachment (WPE) in the southwest USA. Each WPE factor is indicated in a box. An arrow represents a direct impact from one factor to another. A plus (minus) sign indicates an increase (decrease) of the process inside the box as a result of the factor connected to it with an arrow.

These sediment-vegetation interactions create positive feedback loops that contribute to the development of environments more favorable for shrubs than desert grasses (e.g., [66,67,69,80,85]).

WPE has also been related to other indirect factors. Domestic herbivores and native small mammals and insects consume and disperse the seeds of woody plants. In regions where shrubs encroach grasslands, the allelopathic effects of shrubs on grasses may create a positive feedback mechanism for shrub encroachment by inhibiting the establishment of grasses around shrubs (e.g., [82]). Periodic multi-year droughts [64,88], elevated atmospheric CO_2, and interspecific competition have been identified to be potential contributors to WPE [8,14,71,86,93].

Bahre and Shelton [9] and van Auken [92,93] argued that links between historical climate variability since the 1870 s and WPE in semiarid grasslands have been weak. However, there are growing concerns that contemporary and future climate change might increase rates of WPE [2,93], as drier summers in the southwest US predicted by Global Climate Models (GCMs) [28,30] may accelerate the loss of grass species vulnerable to drought, while more drought-tolerant shrubs survive (e.g., [8,41]).

Several numerical models have been developed to investigate WPE. Peters [71] developed an individual plant-based gap dynamics model (ECOTONE) that simulates recruitment, growth, and mortality of individual plants on a small plot scale over annual time steps, governed by probabilistic rules of annual seed production, recruitment, and establishment. ECOTONE was used to examine the influence of soil texture and climate change on grass and shrub composition in central New Mexico, US. When two dominant soil textures, sandy loam and loamy sand were used in ECOTONE, shrubs were predicted to coexist with black grama grass (*B. eriopoda*) on loamy sands, while shrubs were virtually absent in sandy soils, which instead were dominated by grasses. By providing more rainfall during the growing season, the GCM results used by Peters [71] favored grass vegetation over shrubs.

Logistic growth models have also been used to investigate transitions between grass-shrub ecosystems and vegetation coexistence (e.g., [32,34,68]). Okin et al. [68] assumed grass to have a competitive advantage over shrub vegetation. In order to incorporate the effect of grazing in the coupled system, grass carrying capacity was estimated as an increasing function of grass biomass, implying that loss of surface soil resources with loss of grass leads to lower carrying capacity. Despite the assumption of competitive advantage of grasses over shrubs, the model illustrated how a small change in grass mortality due to climate change and grazing could cause an abrupt transition from a grassland to shrubland state. When shrub vegetation is assumed to have a competitive advantage, a similar model yields bistable dynamics due to fire-vegetation feedbacks [32,34].

Ravi and D'Odorico [79] developed a spatially explicit cellular automata (CA) model of grass and shrub dynamics. In their model each cell can exist in a discrete state of grass, shrub (live or burned), and bare soil. The model operates spatially based on annual empirical probabilities of: grass-to-bare soil conversion due to grazing pressure, shrub establishment from neighboring shrub cells, shrub establishment due to seed dispersal by herbivores, fire ignition, and probability of grass seed dispersal. To represent the effects of islands of fertility, available resource in each cell is simulated by removing resource on grazed and burned cells and redistributing them to neighboring cells conditioned on plant type. Shrub vegetation receives more resource than grass due to its higher sediment trapping efficiency. In the absence of periodic fires, the model showed that, while overgrazed desert grasslands may shift towards a shrubland state over a period of 100–150 years, shrub encroachment can be reversed in its early stages if connectivity among grass patches can be maintained [79].

Stewart et al. [88] developed a modeling framework for spatially distributed simulations of coexisting plant types at annual time steps. Amount of soil resource (water and nitrogen) is conserved in each grid cell through vertical and horizontal fluxes and local production (e.g., propagules). Spatial interactions among cells are conditioned on the connectivity of vegetated cells. Biomass growth is calculated empirically as a function of resource limitation. Stewart et al. [88] reproduced the impact of 1950 s drought on grass biomass in central New Mexico, and underscored the role of connectivity of vegetated and bare soil patches as an emergent property of the system.

While significant progress has been made using models to understand WPE, three related research questions still remain to be addressed in regions where WPE is on-going: (1) what are the relative contributions of grazing, fire, and seed dispersal by herbivores on WPE, and how can these factors can be implemented in models? (2) How does the rate of WPE and resulting spatial patterns of woody plants depend on initial woody plant distribution in a region? (3) What is the potential effect of climate change (increasing aridity) on WPE? While the spatially-explicit models mentioned above are useful for developing field-testable hypothesis on WPE, representation of local ecohydrologic processes (e.g., soil moisture, plant water stress, plant growth) that are fundamentally important in plant life cycle processes are either carried out implicitly at annual time steps without explicit partitioning of rainfall into the components of water balance, or neglected entirely. Predicting WPE under a changing climate in semiarid environments requires an ecohydrological framework driven by natural storm characteristics, temperature, and solar radiation in addition to plant life history processes [34,97].

In this study we address the research questions posed above in an active shrub encroachment site in the Sevilleta National Wildlife Refuge (SNWR) using the *Cellular Automata Tree-Grass-Shrub Simulator* (CATGraSS) ecohydrology model [23,98]. We modified CATGraSS to include grazing, fires, and seed dispersal by herbivores using relatively simple algorithms. We systematically examined the individual and interactive effects of these algorithms on WPE and resulting spatial patterns of vegetation in numerical model experiments run in three steps: (1) model spin-up, (2) encroachment experiments from 1861 to 2010, and (3) future climate change experiments. We used the *Advanced WEather GENerator*, AWE-GEN [37,38,52] to represent the historical climate regime and statistically downscale Global Climate Models (GCMs) data to drive CATGraSS. In what follows we first introduce CATGraSS and proposed model improvements, followed by description of the field site, model simulations, and results.

2. Models

2.1. CATGraSS

CATGraSS represents the spatial distribution of elevation, soil texture, and vegetation type using a regular grid of cells. Topographic information for the model is retrieved from a *Digital Elevation Model* (DEM). A vegetation grid is used above the DEM with a finer resolution. Each vegetation cell can hold a single *Plant Functional Type* (PFT), hereafter denoted by X (X is G for grass, SH for shrub), or can remain empty (i.e., bare soil, B). The model combines the functionality of a simplified *Dynamic Global Vegetation Model* (DGVM), which includes the dynamics of local water balance, plant life processes (productivity, carbon allocation), and plant mortality (e.g., [87]) at each model grid cell with a cellular automata (CA) component for probabilistic plant establishment driven by plant seed dispersal length and water stress (e.g., [53,54,94]). Plant mortality is treated probabilistically and results from drought stress, plant aging (for woody plants),

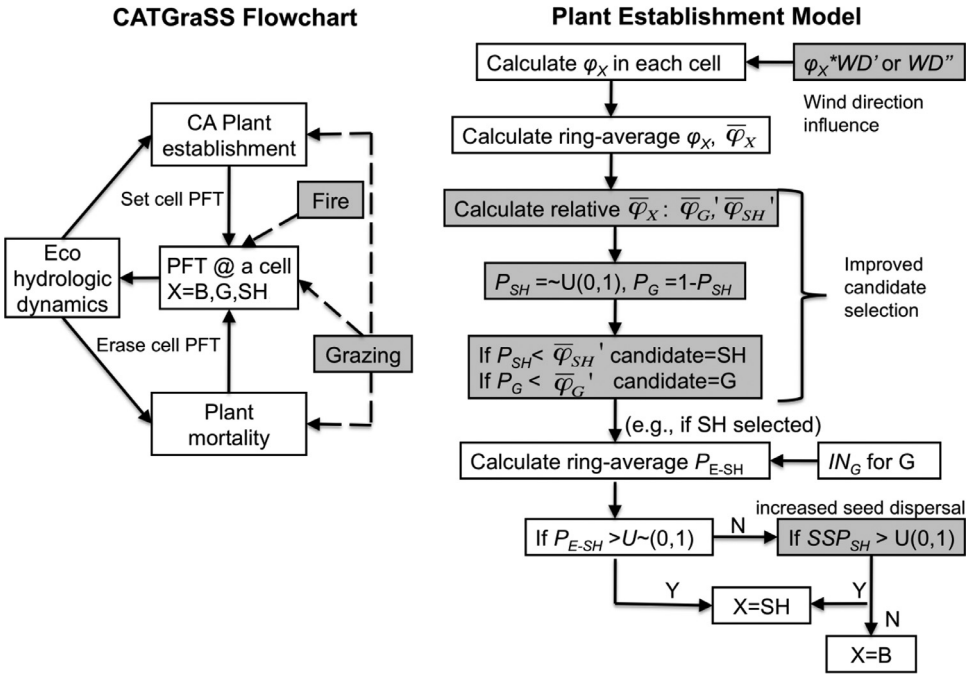

Fig. 3. CATGraSS flowchart (left panel) illustrates the interactions among plant establishment, mortality, and ecohydrologic components and the proposed fire and grazing components used in this study. *X* is the variable used to designate the plant functional type (PFT) at a model cell and can be bare (*B*), shrub (*SH*), and grass (*G*). The flowchart in the right panel presents the integration of the steps for plant establishment in the original model (white boxes) and the proposed improvements (gray boxes) as part of this study.

and disturbances. Here we only discuss formulations used in the CA component of CATGraSS, for a full description of the model see Zhou et al. [98] and Caracciolo et al. [23].

Fig. 3 (left panel) presents a flowchart of CATGraSS components. CA rules for plant establishment set a PFT at a cell. Plant mortality erases an existing PFT as a result of death due to age and disturbances. Both processes use an index of plant water stress provided by the ecohydrologic dynamics model, which tracks soil moisture and plant biomass dynamics. Grazing and fires reduce vegetation biomass at a cell, while grazing also influences local mortality and establishment probabilities. In this study CATGraSS is implemented only for shrub and grass PFTs, without considering trees, as they are not observed in this grass-shrub ecotone.

For computationally-efficient modeling of plant ecohydrologic dynamics in large regions (e.g., water balance, phenology) grid cells are grouped into topographic bins, based on their slope and aspect values within narrow ranges. At each bin a daily transpiration factor (f_T) is used to scale daily potential transpiration T_{max} of a flat surface, to the T_{max} of a topographic bin. In the model f_T is calculated based on latitude, slope, and aspect characteristics of the bin as a pre-processing model step from well established relationships of solar radiation physics [4,98]. To reduce data requirements and keep the model simple, the potential evaporation for bare soil, E_b, is taken as a fraction (f_b) of the maximum grass transpiration rate, $T_{max\text{-}G}$ (i.e., $E_b = f_b \cdot T_{max\text{-}G}$).

CATGraSS continuously simulates the root-zone water balance and plant dynamics for each PFT and their seedlings within each topographic bin, driven by spatially uniform daily rainfall and T_{max} calculated for each PFT using the Penman–Monteith equation. The model has a global time that advances based on the summation of generated storm and inter-storm durations. Other processes such as plant establishment, mortality, and fires are iterated annually using their respective probabilities. Modeled soil water and plant variables include soil moisture, evapotranspiration, net primary productivity (NPP), and live, structural and dead biomass allocated to aboveground and belowground pools simulated on a daily time-step [23,98].

The probabilistic plant establishment algorithm runs in the beginning of each growing season at each bare soil cell. Establishment probabilities are calculated for each PFT based on seed availability and plant water stress. Grasses in this system reproduce by rhizomes and by seeds, allowing them to increase in size and number over time [29,73]. Our modeling approach incorporates both of these mechanisms of reproduction. We make the assumption that grass seeds are available for growth everywhere in the model domain. If grass establishes at an empty cell the increase in the size of grass is related to the available biomass [98].

Shrubs, which only reproduce by seed, are assumed to provide seeds to their first ring of surrounding neighboring cells (8 cells); [53,94]. Seedlings, however, cannot produce seeds until they become mature [53]. A shrub is assumed to mature and disperse seeds in 18 years [27] while their maximum longevity is assumed to be 600 years [15]. We postulate that the probability of establishment ($P_{E\text{-}X}$) of a PFT at a bare soil patch as a result of seed dispersal can be related to the ecohydrological condition of neighboring plants. In order to measure plant condition, CATGraSS uses a plant live index, φ_X [−], defined as the complement to an index of water stress, WS_X [−]:

$$\varphi_X = 1 - WS_X \tag{1}$$

where WS_X is calculated as the sum of the mean inter-storm water stress, ξ, multiplied by its inter-storm duration (TB, [T]), divided by the growing season length, TG [T], based on Porporato et al. [76] and modified by Istanbulluoglu and Bras [51]:

$$WS_X = \frac{\sum^{N_{is}} (\xi \cdot T_B)}{T_G} \tag{2}$$

where N_{is} is the number of inter-storm events during a growing season. φ_X of all mature shrub neighbors in the first ring (I) of a bare soil cell is calculated at the end of each growing season and averaged to use as the probability of shrub establishment in the bare cell:

$$\overline{\varphi_{SH}} = \sum \varphi_{SH}^{I}/8 \tag{3}$$

Since we assume grass propagules are abundant everywhere in the basin [53,94], the mean live index for grass, $\overline{\varphi_G}$ is taken as the average live index of all grass cells within the modeled domain located in the same slope and aspect (*S-A*) group of the bare cell [98].

A component in the establishment probability calculation relates to allelopathy, defined as a biological process by which a plant produces one or more biochemicals that limit the growth, survival, and reproduction of another plant. Knipe and Herbel [56] analyzed the germination and growth of semiarid grassland species treated with aqueous extract from creosotebush. Their data indicated that the germination of grasses (e.g., black grama) is significantly reduced, while shrub species were not affected. Therefore, based on the work of Knipe and Herbel [56], in our application of CATGraSS in central New Mexico, we assume that the allelopathic effects of creosotebush influences grasses, but that grasses are not allelopathic. Allelopathy is integrated in CATGraSS by using an inhibitory factor, IN_G. A cumulative inhibition factor is obtained as the product of a single shrub inhibition factor on grass (IN_G) and the number of shrub cells in the first ring (N^I) of a grass cell.

The establishment probabilities of grass and shrub functional types on a bare soil cell are:

$$P_{E-G} = \min\left(\frac{\overline{\varphi_G}}{IN_G \cdot N^I}, P_{E-G,\max}\right) \tag{4a}$$

$$P_{E-SH} = \min(\overline{\varphi_{SH}}, P_{E-SH,\max}) \tag{4b}$$

In the equations above, maximal establishment probability values, $P_{E\text{-}X\text{-}max}$ [−], are introduced as an upper limit to prevent unrealistically fast colonization rates by each PFT in a bare soil cell during favorable conditions [53,94].

Plant mortality removes a plant type from a cell, and sets the cell status to bare. Plant mortality is treated probabilistically and operates at the end of the growing season. Annual probability of plant mortality is obtained as the sum of three probabilities: mortality due to drought stress ($P_{Md\text{-}X}$), plant aging ($P_{Ma\text{-}X}$), and local disturbance ($P_{Mb\text{-}X}$) such as grazing:

$$P_{M-X} = \min(P_{Md-X} + P_{Ma-X} + P_{Mb-X}, 1) \tag{5}$$

where $P_{Md\text{-}X}$ [−] is calculated as WS_X minus a PFT-specific drought resistance threshold value, θ_X [94], while $P_{Ma\text{-}X}$ is only modeled for woody plants (e.g., tree and shrub), as a piecewise function of plant age [54]. We relate plant mortality due to plant aging ($P_{Ma\text{-}X}$) to the age of each shrub using the formulation of Jeltsch et al. [54] that linearly increases probability of mortality from 0 to 1 when the age of an individual plant is greater than half of its defined maximum age ($T_{Pmax\text{-}X}$). The model of Jeltsch et al. [54] neglects age-dependent mortality when plant age is younger than half of its $T_{Pmax\text{-}X}$. Finally $P_{Mb\text{-}X}$ [−] is introduced as background probability that could incorporate the influence of disturbances. A plant is removed when $P_{M\text{-}X}$, calculated for each PFT from Eq. (5) , is greater than a uniformly distributed random number between 0 and 1 ($U\sim(0,1)$), $P_{M\text{-}X} > U\sim(0,1)$.

2.1.1. Model improvements

In this study encroachment factors including grazing, fire, and effects of herbivores on seed dispersal are introduced in CATGraSS (Fig. 3, left panel). A new plant selection procedure and the role of wind direction are implemented within the existing plant establishment procedure (Fig. 3, right panel). First we describe the improvements in the plant establishment component followed by the explicit representation of factors that may cause shrub encroachment.

WPE is tightly related to plant competition for space rather than coexistence [71]. In the original CATGraSS model while the probability of plant establishment has been related to plant water stress, the initial plant selection for the "candidate" PFT (shrub or grass) for establishment was performed at random. This algorithm does not prioritize the PFT that has the highest live index among the competing PFTs to be more competitive for the initial selection procedure for the candidate PFT. To improve this, a new plant selection procedure is implemented in CATGraSS, based on a relative comparison of the live indices of the competing shrub and grass vegetation types (Fig. 3, right panel).

The plant establishment processes in the improved model include the following two major steps. In each iteration of the algorithm, first all bare soil cells are identified and in order to select the "candidate" PFT for an unoccupied bare soil patch, a relative live index for shrub and grass vegetation types scaled to the combined live index of both vegetation types is calculated at each bare soil cell as:

$$\overline{\varphi'_{SH}} = \overline{\varphi_{SH}}/\overline{\varphi_C} \tag{6a}$$

$$\overline{\varphi'_{G}} = \overline{\varphi_G}/\overline{\varphi_C} \tag{6b}$$

where the combined live index is $\overline{\varphi_C} = \overline{\varphi_{SH}}/\overline{\varphi_G}$.

Following the calculation of the relative live indices for shrub and grass vegetation types at each bare soil cell, a shrub probability of selection, P_{SH}, is generated using a uniform distribution $\sim U(0,1)$ and, simultaneously, the probability of grass selection, P_G, is set equal to $1-P_{SH}$ as either shrub or grass will be selected as the number of trials grow (i.e., $P_{SH}+P_G = 1$). Then, if $P_{SH} < \overline{\varphi_{SH}'}$, shrub is selected, otherwise grass is selected (i.e., $P_G < \overline{\varphi_G'}$). This algorithm gives a higher probability of selection for a PFT that has a higher relative live index.

Second, once a PFT is selected, the establishment probability $P_{E\text{-}X}$ is calculated for the selected PFT and compared with a uniformly distributed random number between 0 and 1 ($\sim U(0,1)$). If $P_{E\text{-}X}$ is greater than $U\sim(0,1)$, the selected PFT in the first step is placed in the cell, otherwise the cell is left bare for a year (Fig. 3, right panel).

In the original CATGraSS model plants disperse seeds equally in all directions. It has been argued in the literature that the prevailing wind direction in a region may impact the likelihood of plant establishment along its track [63,92]. We represented this phenomenon by multiplying the plant live index, φ_X, by a pair of amplifying coefficients named *wind direction factors, WD* ($WD > 1$). We assumed that at a given cell the prevailing wind direction can be either of the four cardinal (N, S, E, W) or four ordinal (NE, SE, NW, SW) directions across a cell. The proposed algorithm first assigns wind directions at each cell and identifies all model cells in the upwind direction of an unoccupied cell within the first (or more) ring(s) of neighbors, depending on the number of rings used to represent the seed dispersal range. The φ_X of vegetated cells located in the immediate upwind direction of a bare soil cell are multiplied by WD', increasing their probability of establishment at the bare soil cell. In the case of ordinal wind directions, in addition to using WD' at the immediate upwind cells ($\varphi_X \cdot WD'$), cells with one of the vector components pointing in the direction of the unoccupied cell are multiplied by WD'' ($WD'' < WD'$). These factors amplify the probability of establishment of the PFTs along the prevailing wind direction (Fig. 3, right panel).

The modified plant selection process and the role of wind direction are used in all CATGraSS simulations presented in this paper. In the following section algorithms developed specifically to represent the direct and indirect impacts of grazers on spatial vegetation dynamics are discussed as potential factors promoting shrub encroachment.

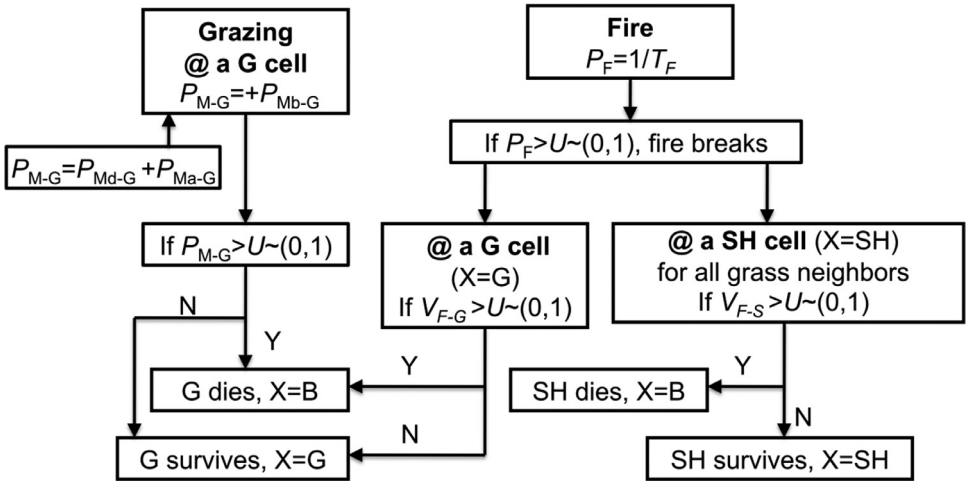

Fig. 4. Flowcharts for the modeling of spatial dynamics of plant functional types (PFTs) as a result of probabilistic rules for grazing and fire in the cellular automata model.

2.1.2. Representation of the factors of encroachment

2.1.2.1. Grazing. The influence of grazing is limited to grass in the model as herbivores in central New Mexico graze primarily herbaceous vegetation [92,93]. Two direct effects of grazing are considered. First, loss of grass biomass through grazing herbivores is represented by increasing the first-order decay coefficient of live grass biomass, $k_{sg\text{-}G}$, in the model (i.e., $dB_l/dt \sim -k_{sg\text{-}G}\cdot B_l$) (Eq. 10 in Zhou et al. [98]). Second, grazing is assumed to elevate the constant background probability of mortality due to disturbances ($P_{Mb\text{-}G}$) in Eq. (5), similar to the probability of grazing pressure in Ravi and D'Odorico [79]. Following the CATGraSS mortality rules, grass dies and the cell is set as bare when $P_{M\text{-}G}$ is greater than a $U\sim(0,1)$, $P_{M\text{-}G} > U\sim(0,1)$, else grass is kept on the cell for the next growing season (Fig. 4).

2.1.2.2. Fire

Fire implementation in the model resembles a Bernoulli process with equal probability of fires, P_F, occurring each year. P_F is defined as $1/T_F$, where T_F is the fire return period. In each model year, if P_F is greater than a generated uniformly distributed random number between 0 and 1, $P_F > U\sim(0,1)$, a fire is triggered in the modeled domain (Fig. 4). P_F is likely to increase with the amount of grass fuel available on the ground [39] and decrease with soil wetness. These factors can be incorporated into the model. For example, P_F may be positively related to the number of grass cells within the modeled domain [53] or reduced in anomalously wet years. However, in order to examine the effects of fire frequency independent of other state variables in the model, we kept P_F as an independent parameter, which we varied based on published T_F values for the study region.

Occurrence of a fire does not ensure the consumption and death of all the plants in a region since vulnerability of grass and shrub plant types to fire can be different. We address such differences using a vulnerability to fire parameter, $V_{F\text{-}X}$, introduced by Accatino et al. [1]. $V_{F\text{-}X}$ is defined for each PFT and ranges between 0 (no vulnerability to fire) and 1 (no resistance to fire). When a fire is simulated in the model domain, $V_{F\text{-}X}$ of each plant is compared against a uniformly distributed and independently generated random number at each cell. In a grass cell, grass vegetation burns if its vulnerability to fire, $V_{F\text{-}G}$, is greater than $U\sim(0,1)$ (Fig. 4). Over the model domain $V_{F\text{-}G}$ gives the fraction of grass burned by a single fire event in the domain. In the case of shrubs, however, the comparison between $V_{F\text{-}S}$ and a $U\sim(0,1)$ is repeated as many times as the number of neighboring grass cells in the first ring of a shrub cell. This implies that the greater the number of neighboring grass cells the higher the probability of a shrub cell to be killed by a fire.

2.1.2.3. Seed dispersal caused by animals

The introduction of herbivory in the study area since 1860 has increased the chances of arrival of seeds at bare soil patches from any direction and distance from a seed source as a result of seed dispersal by grazers (e.g., domestic cattle) that can carry and disperse seeds in all directions [92,93]. In order to incorporate this additive effect of herbivores a spread of seed probability (*SSP*) is introduced in the CA component of the model. The *SSP* parameter is only used for shrub vegetation as grass seeds and rhizomes are assumed to be available in the entire area in abundance. *SSP* is introduced as the final step in the seed establishment process to provide an additional opportunity for a "candidate" shrub plant to establish at a bare soil site, if the first trial experiment for establishment fails in the last step of the establishment procedure (Fig. 3, right panel). If $SSP > U\sim(0,1)$, shrub is placed in the cell, otherwise the cell is left bare for a growing season.

2.2. AWE-GEN and stochastic downscaling

The *Advanced WEather GENerator*, AWE-GEN [52] is a statistical model that can reproduce statistical properties of weather variables including precipitation, cloudiness, shortwave radiation, air temperature, and wind speed observed over a range of time scales. A methodology for stochastic downscaling of GCM data was also introduced to AWE-GEN [37,38]. In this study AWE-GEN is used to generate weather data to force model spin-up and historical encroachment experiments, and to downscale GCM outputs for future climate change simulations. AWE-GEN was preferred in historical simulations because of lack of long-term observations at the study site. The stochastic downscaling method uses a Bayesian approach to weight climate model realizations [37,89] and develop probability distributions for *factors of change* (FOC) representative of the ensemble of GCM projections. FOCs of weather variables from climate models are calculated as ratios or "delta" differences of GCM climate statistics for historical and future periods at different aggregation periods (24, 48, 72, 96 h). The median value of FOC is used to update AWE-GEN parameters assuming stationary climate for any considered future period. Updated AWE-GEN parameters are used to simulate hourly time series of hydro-climatic variables to represent future climate. AWE-GEN is also capable of simulating transient climate change by varying statistical parameters of weather variables obtained from GCMs

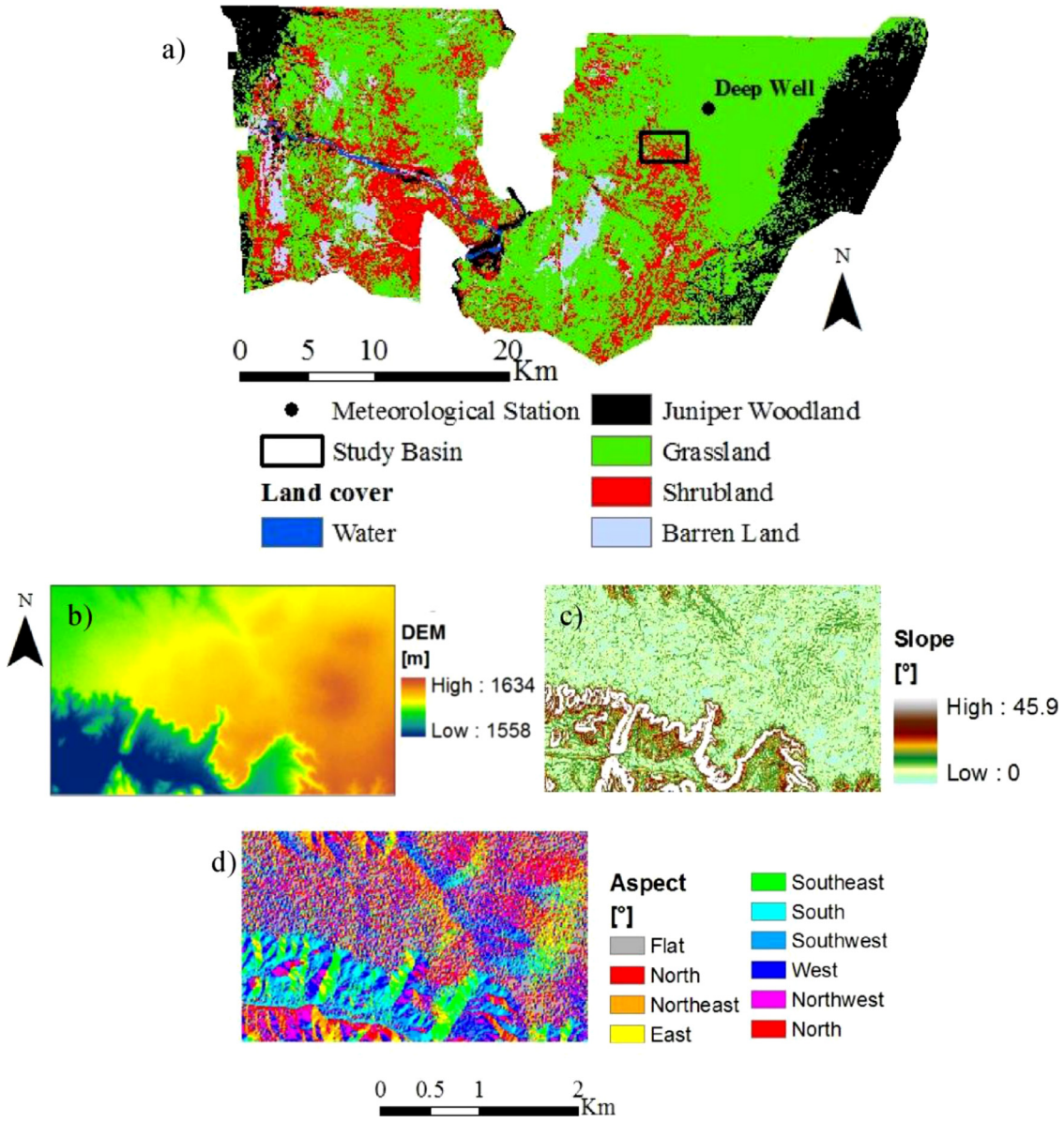

Fig. 5. Study site in central New Mexico: (a) the land cover map of the Sevilleta National Wildlife Refuge (SNWR, source: NLCD 2006 map), overlain by the watershed boundary of the study site and the Deep Well weather station; (b) basin topography represented by a 10-m IFSAR DEM; and maps of (c) slope and (d) aspect derived from the DEM.

gradually with time, which is the preferred approach for stochastic downscaling used in our study [23]. Since CATGraSS operates at daily (or inter-storm when desired) time scales, the generated hourly precipitation data by AWE-GEN are then aggregated to daily totals while other hourly weather variables are averaged over a day before using in CATGraSS. Daily T_{max} is calculated with the Penman–Monteith equation using the daily data for historical and future climate change simulations.

3. Modeling study site

3.1. Site description

We studied shrub encroachment in a rectangular domain located within the Sevilleta National Wildlife Refuge (SNWR) (34°24′ N, 106°59′ W), in the northern Chihuahuan Desert of the Rio Grande Valley, approximately 80 km south of Albuquerque, New Mexico, USA. The selected site is at the northern range boundary of creosotebush (*Larrea tridentata*) of a region of vegetation transition (ecotone) where shrub encroachment has occurred [33] since the middle of the 19th century [19,92]. Fig. 5a shows the land cover map of the SNWR, obtained from the National Land Cover Database (NLCD) 2006 in 30 m resolution (http://www.mrlc.gov/nlcd06_data.php). The Northeastern quadrangle of the SNWR clearly shows a dramatic encroachment front of creosotebush into native desert grassland. The selected study site is indicated by a rectangular outline. It has an area of 7.34 km^2 (2.1 × 3.5 km), and mainly contains C_4 perennial grasses: blue grama (*Bouteloua gracilis*), black grama (*B. eriopoda*) and galleta (*Pleuraphis jamesii*) grass; and the evergreen C_3 shrub creosotebush, with a current spatial coverage of 42% (Fig. 5a).

A 10-m *Interferometric Synthetic Aperture Radar* (IFSAR) DEM of the SNWR (Fig. 5b) (source: http://sev.lternet.edu) was used to obtain local slope and aspect of the topography for solar radiation calculations. The site has an abrupt change in elevation from a river valley on the southwestern quadrangle of the area with steep

Table 1
Soil parameters used in the water balance component of the model and parameters for plant mortality, establishment, and fire components.

Parameter		Description	Value		
Soil	β	Coefficient of the hydraulic conductivity power low [−]	13.8[1]		
	k_s	Saturated hydraulic conductivity [mm/h]	42[2]		
	n	Porosity [−]	0.43[1]		
	s_{fc}	Soil saturation degree at field capacity [−]	0.56[1]		
	$I_{c\text{-}b}$	Bare soil infiltration capacity [mm/h]	20[3]		
			Grass	Shrub	Shrub seedling
Vegetation	θ_X	Drought-resistant threshold [−]	0.62[4]	0.80[4]	0.64[4]
	$P_{Mb\text{-}X}$	Background mortality probability [−]	0.01[4]	0.01[4]	0.01[4]
	$P_{E\text{-}X\text{-}\max}$	Maximal establishment probability [−]	0.35[4]	0.2[4]	N/A
	IN_X	Inhibitory factor [−]	1.12[4]	N/A	N/A
	$T_{P\max\text{-}X}$	Maximum age [yr]	N/A	600[5]	18[6]
	P_F	Probability of fire [yr^{-1}]	0.1[7]		
	V_{F_X}	Vulnerability to fire [−]	0.8[8,4]	0.11[8,4]	0.2[8,4]

Source: (1) Laio et al. [58]; (2) Bhark and Small [12]; (3) calibrated based on Gutierrez-Jurado et al. [45]; (4) Calibration; (5) Bowers et al. [15]; (6) Chew and Chew [27]; (7) Parmenter [70]; (8) Accatino et al. [1].

south facing slopes as high as 45.9° to a plateau-like elevated flat surface (Fig. 5c). Aspect map is given in Fig. 5d.

The dominant soil type in the modeled region is sandy-loam (Table 1). Hydrologically active soil thickness is assumed to be limited by the root zone of each PFT, taken as 0.3 m for grass and 0.5 m for shrub vegetation [57]. CATGraSS uses a number of parameters to represent local vegetation dynamics (water balance, biomass production, allocation, and senescence). In this study we used vegetation dynamics parameters directly from Zhou et al. [98] who calibrated CATGraSS at the SNWR, while some of the CA parameters required local calibration as new components were introduced.

CATGraSS simulates water balance and vegetation water stress for each PFT lumped into topographic bins. Topographically similar slope-aspect (*S-A*) groups are developed considering a 6-degree increment for local slope, ranging from 5° to 47° at the site (8 slope classes), and a 30-degree increment for aspect (13 aspect classes), leading to 104 different combinations (*S-A* groups). PFTs are defined using a 5 m-resolution vegetation grid following Zhou et al. [98].

3.2. Historical weather data

Hourly weather data are required to characterize statistical properties of the local climate at the study site for both historical (spin-up and encroachment experiments) and future climate simulations. Local weather data including hourly precipitation, temperature, wind speed, relative humidity, incoming shortwave radiation, and actual vapor pressure are available at the Deep Well weather station between 1990 and 2008, located slightly northeast of our modeling site (http://sev.lternet.edu/data/sev-1) (Fig. 5a). The mean annual precipitation (MAP) at the site is 249.1 mm, with more than half of the precipitation falling during the monsoon season (3-month wet season from July to end of September) characterized by high-intensity rainfall events. Fall, winter, and spring rainfalls (9-month dry season) are driven by broad-scale frontal systems [42,45]. The mean monthly temperature ranges between 2.5°C in January and 25°C in July. The prevailing wind direction is from southeast to northwest (http://sev.lternet.edu/data/sev-079). The observed weather data at the Deep Well station are used to (1) characterize the stochastic nature of weather variables to use in the spin-up and encroachment experiments in AWE-GEN, and (2) estimate monthly FOC values of the observed historic climate with respect to GCM outputs to parameterize climate change in AWE-GEN.

Representing historical climate trends, if any, is critical for the encroachment simulations. The Deep Well weather station has only limited data for 18 years, not sufficient for trend analysis. Longer time series of annual precipitation and mean temperature were obtained from the Socorro County (NM) station (SCS) from 1893 to 2010 (source NOAA - *National Oceanic and Atmospheric Administration*) (Fig. 6). Annual precipitation and temperature data clearly show drier conditions from early 1940 s to late 1950 s (referred to as the 1950 s drought) while the temperature record seems to show periodicity likely related to the Pacific Decadal Oscillation [64]. Despite the 1950 s drought, studies did not show any significant climate change trends in the last 150 years in central New Mexico [74], and future projections for the summer monsoon indicate higher interannual variability but no directional trends in precipitation for this region [46]. The Mann–Kendall test with a significance level (α) of 0.01 applied to the annual, wet and dry season time series of Socorro did not show any statistically significant trends. While we develop a large set of encroachment simulations that test grazing, fire, and seed dispersal effects of herbivores using generated stationary climate from AWE-GEN, observed climate data (Fig. 6) are also used for a small set of model scenarios for comparison.

3.3. Model simulations

Model experiments are carried out in three steps: model spin-up, encroachment, and future climate change experiments. During the model spin-up, we ran CATGraSS for 5000 years without encroachment factors in order to reproduce the hypothesized shrub and grass percentages and their distribution in 1860. The model is started with an initial cover condition of equally distributed grass,

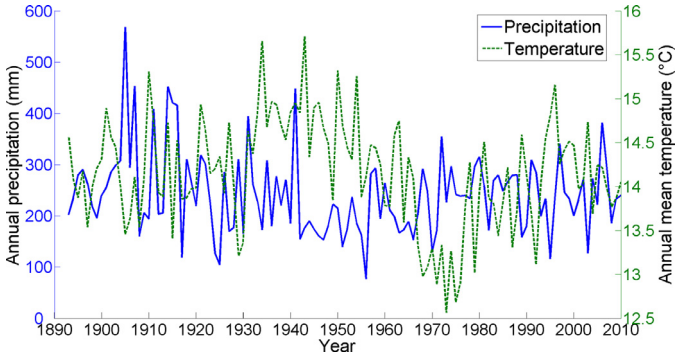

Fig. 6. Annual precipitation and annual mean temperature measured at Socorro County station (SCS), from 1893 to 2010 (*source*: U.S. Historical Climatology Network, www.ncdc.noaa.gov/oa/climate/research/ushcn/ushcn.html).

shrub, and bare soil (each with 33% cover) randomly assigned across the model domain. Probabilistic establishment, mortality, and vegetation fire vulnerability parameters are calibrated during the spin-up simulations. The resulting field of vegetation cover is then used in the encroachment experiments.

Encroachment experiments aim to reproduce the shrub encroachment from 1861 to 2010 using grazing, fire, and seed dispersal algorithms individually, two-factor combinations, and all together with a range of parameter values. Modeled vegetation outputs are compared against the current patterns and percentage of shrub vegetation in Fig. 5a. Among encroachment simulations, a scenario that reasonably reproduces historical shrub encroachment in the region is selected and used in the future climate change experiments.

Both spin-up and encroachment experiments have been driven with generated stationary weather data using AWE-GEN parameterized based on statistical properties of the 19 years (1990–2008) of observed weather data at Deep Well.

In order to generate future climate, eight GCMs (CCSM3, CSIRO-Mk3.5, ECHAM-5, IPSL-CM4, CGCM3.1, GFDL, INGV, MIROC3.2) from the IPCC-4AR [62] are used to produce a transient climate change scenario for ninety years (2010–2100). The selection of models is based on availability of modeled daily precipitation time series as the main constraint, and relative independence among the models (different development groups). The GCM realizations here selected, which correspond to the A1B emission scenario [50], exhibit a large spread of modeled climate variables, underlining the inherent uncertainties in climate model predictions. This is particularly evident for precipitation where FOCs are substantially different among the models, while changes in air temperature are generally more coherent. The stochastic downscaling is applied using Deep Well weather station data.

In this study the 1990–2000 period is used as the control period for the climate change simulations. The medians of the probability distributions of monthly FOCs are used to estimate climate statistics for the central years (2055 and 2090) of the periods 2046–2065 and 2081–2100, respectively, with respect to the central year of the control period. The central year of the control period is represented by the mean monthly statistics calculated for the 1990–2000 period for precipitation and temperature. FOCs for all of the other years in the period 2011–2100 were linearly interpolated between the downscaled years (1995, 2055 and 2090) using the same methodology presented by Burton et al. [22] to obtain transient climate change scenarios (see also [23,38]). In this way, ninety sets of AWE-GEN parameters (one for each year) are estimated and used to generate weather data. The previously discussed stochastic downscaling procedure has been carried out only to generate precipitation and air temperature. Generated future precipitation and temperature are used in AWE-GEN for estimating solar radiation, and generating relative humidity and wind speed for future climate [38].

Downscaled precipitation and temperature show changes in the future. In the observed 2001–2008 period, the mean wet season (July–September growing season) precipitation is 104.5 mm, and dry season precipitation is 149.1 mm (MAP equal to 253.6 mm). In the 2091–2100 period, however, the mean wet season precipitation is predicted as 89 mm (~14.5% decrease) and the mean dry season precipitation is predicted as 159 mm (~6.7% increase), with a MAP of 248 mm. The mean inter-storm period, T_b, is predicted to increase from ~80 h in 2001–2008 to ~84 h in 2091–2100, the mean storm depth is predicted to slightly increase from 2.32 mm in 2001–2008 to 2.36 mm in 2091–2100, while the mean storm duration, T_r, is predicted to decrease from 70 min. to ~50 min. Therefore, the future climate predicted by the model is characterized by less frequent but more intense storms. Annual air temperature is projected to increase ~4.2°C from 2010 to 2100. Reduced rainfall and warmer temperature are projected to cause more arid conditions in this region by the end of the century (e.g., [30]).

4. Results

4.1. Initial conditions and spin-up simulation

The percentage and pattern of shrub distribution in the region prior to encroachment are not known, although studies confirm that shrub cover in this region was very low before encroachment that started ~150 years ago [6,18,55,72,79]. In order to calibrate the model, we quantitatively interpreted this statement as ~4% shrub cover in the study site in 1860. Based on image analysis of aerial photographs, Laliberte et al. [59] reported 9% shrub cover in southern New Mexico in 1937. Because our site is further north we believe a smaller value for shrub cover is justified.

Two different spatial patterns of shrub distributions with 4% shrub cover in the domain were used as initial conditions for encroachment simulations. The first initial condition, named *E1*, was developed following Knapp et al. [55] who suggested that the shrub line moved gradually from south to north in the region. This is represented by randomly placing shrub cells that gradually decrease from a ~8% coverage in the southern boundary of the domain to 0% shrub at the northern boundary, with a domain-averaged coverage of 4%. The second initial condition, named *E2*, is developed through limited model calibration in the spin-up simulation.

Table 1 reports vegetation parameters used for simulating plant establishment, mortality, and fire, mostly identified through model calibration to obtain 4% shrub cover in the domain. In the spin-up simulation we have not targeted any spatial patterns in the modeled shrub distribution, such as an encroachment front or cluster distribution of shrubs, as spatial patterns of shrubs are also unknown in the region in the 19th century.

An annual probability of fire, P_F, of 0.1 is used in the model (return period, T_F, equal to 10 years) in accordance with Casagrandi and Rinaldi [24] for pre-encroachment conditions. Vulnerability to fire for each vegetation, $V_{F\text{-}X}$, (shown in Table 1) is set to 0.8 for grass (i.e., 80% of grass in the domain burns in every 10 years on average), to 0.11 for mature shrubs and 0.2 for young shrubs after a sensitivity analysis carried out using the value ranges reported by Accatino et al. [1]. Grasses are more vulnerable to fire than shrubs, while shrub seedlings are more vulnerable to fire than mature shrubs [1]. The background probability of grass and shrub mortality due to disturbances and diseases, P_{Mb}, is very low in this system [73], considered constant, and set to 0.01.

Initially, the factors of allelopathy IN_G, (Eq. (4a)) and wind direction (WD′ and WD′′) were first not considered by setting these parameters to 1. This led to the disappearance of shrubs in the domain in the spin-up simulations. Different simulations were carried out by gradually increasing IN_G by 0.02. The IN_G value was chosen as 1.12, which suggests a relatively small allelopathic influence of shrubs on grasses. In order to take into account the influence of wind direction on vegetation pattern, the wind direction factors, WD' and WD'', were introduced as previously described in the Section 2.1.1 . Values of WD' ranging from 1.5 to 5, and of WD'' from 1 to 4, at 0.5 increments, have been considered for shrub, and they have been calibrated in order to obtain shrub cover equal to 4% in the domain. The final selected values are 2 and 1.5 for WD' and WD'', respectively.

The final vegetation distribution after 5000 years of stochastically-driven CATGraSS runs using the selected parameters (i.e., *E2*) and the time series of percent coverage of PFTs in the study site over the modeled duration are shown in Fig. 7a and b, respectively. The vegetation percentages obtained at the end of the simulated 5000 years (i.e., 1860) are: 4% shrub, 86%

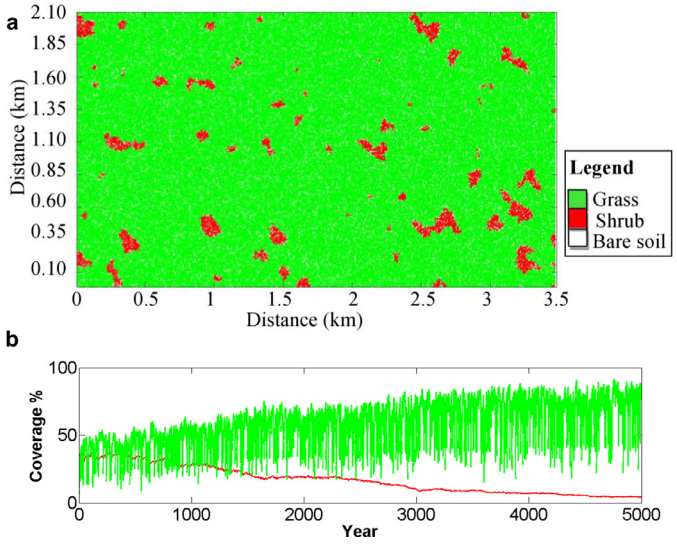

Fig. 7. (a) Final Vegetation distribution after 5000 years in the spin-up simulation (*E2* initial condition, in which shrubs occur in clusters or patches), (b) time series of percent coverage of plant functional types (PFTs) in the modeled study area.

grass, and 10% bare soil. The spatial distribution of shrubs follows a cluster pattern without any evident influence of the topography on vegetation pattern. Cluster distributions of woody plants have been observed in semiarid ecosystems globally [59–61,84]. Evidence for pre-encroachment spatial patterns of shrubs does not exist. However cluster patterns used as initial condition in our model provide an opportunity to investigate the sensitivity of our model to two end-member initial conditions, one with random distributed shrubs (i.e., *E1*) and the other with relatively large clusters (e.g., representing refugia) (i.e., *E2*), while both have identical areal cover fraction of shrub vegetation.

The shrub time series in Fig. 7b shows a decreasing trend with very little year-to-year fluctuation, while grass cover persistently increased over time. The highly variable nature of grass cover is driven by the inter-annual fluctuations in precipitation, and has a lag-1 autocorrelation coefficient of 0.75. Grasses develop an overall higher water stress than shrubs in the simulations and they have a lower drought resistance [8]. As a result, a relatively large fraction of grasses die during dry years, but they also grow back rapidly in the following wetter years, from belowground reserves and seeds, both of which are assumed to be available everywhere in the modeled domain.

4.2. Encroachment experiments

4.2.1. Sensitivity analysis of encroachment factors

In the encroachment simulations we ran CATGraSS for 150 years to investigate the roles of fire return period (*F*), grazing intensity (*GR*), and herbivore influence on seed dispersal (*SD*) on shrub and grass patterns by systematically varying these factors. Each factor is first used individually and then in combination. We identified parameter ranges that reproduce the current shrub percentage of ~40% from an initial condition of very low shrub cover equal to ~4% (i.e., *E1* and *E2* (Fig. 7a) initial conditions).

In the first set of simulations we examined the sensitivity of the model to varying conditions of *GR* and *SD* under a historic fire return period, T_F, of 10 years. Using a fixed fire frequency allows us to illustrate the effects of individual factors of *GR* and *SD*. Grazing (*GR*) was introduced at the SNWR region in 1860 ([92], 2009).

The effect of *GR* was represented by two parameters in the model. First, on a daily-basis *GR* reduces the amount of live biomass in the model, by amplifying the decay coefficient of green biomass, $k_{sg\text{-}G}$, from 0.004 d^{-1} in the spin-up simulation to 0.012 d^{-1} in the encroachment simulations, consistent with ranges used for this parameter [65,98]. This $k_{sg\text{-}G}$ value is fixed and used in all of our simulations that involved *GR*. Second, probabilistic plant mortality due to *GR* is introduced by increasing the background probability for disturbance, P_{Mb}, included in the annual probability of plant mortality, P_M (Eq. (5)) [98]. Because of its control on vegetation state in each cell, P_{Mb} was used as a calibration parameter and to examine the influence of grazing. In our sensitivity analysis, we simulated ten different *GR* scenarios that provided constant P_{Mb} values ranging from 0.025 to 0.25 (i.e., 2.5% to 25% chance of annual mortality respectively) with an equal increment of 0.025.

With regard to *SD*, van Auken [92,93] stated that the introduction of animals in the study area from 1860 enhanced the chances that shrub seeds would arrive in a bare soil patch from any distance by the continuous movement of grazers (e.g., [17]). To account for dispersal by grazers within the model framework, we varied the spread of the seed probability parameter, *SSP*, from 0.001 to 0.01 using 0.001 increments. For example, *SSP* equal to 0.01 gives an additional 1% chance of establishing a shrub plant in a neighboring bare soil cell every year. Even if this value is small, its cumulative impact over time can be fairly significant.

To facilitate the comparison of model results with different encroachment factors objectively, we first established a baseline simulation (*BØ*) of 150 years (1861–2010) for both *E1* and *E2* initial conditions. In the baseline simulations the parameter values used are identical to the spin-up model runs (i.e., without encroachment factors). *BØ*, driven by identical climate forcing as other encroachment simulations, is expected to give coverage percentages of shrub and grass similar to those of the initial conditions in 1861.

We present the modeled final percent coverage of shrub and grass vegetation types with *E1* and *E2* initial conditions for each single-factor sensitivity run of the model in Fig. 8a,b,c and d. The model shows high sensitivity to the initial vegetation distribution used in the simulations. In the case of *E1*, with randomly distributed individual shrubs, loss of grass by *GR* leads to a positive feedback to shrub cover, which increased from 4% (base case, P_{Mb} equal to 0.01) to 38.26% (P_{Mb} equal to 0.25) (Fig. 8a). Under a natural fire regime that creates bare soil patches, grazing herbivores increase seed dispersal probability (*SSP*), which also leads to shrub expansion (Fig. 8b). In the case of *E2*, with initial clusters of shrubs that are developed during model spin-up (Fig. 7a), shrubs are locked in clusters and they show very little response to *GR* and *SD* (Fig. 8c and d), while *GR* naturally leads to loss of grass cover with some step-like behavior (Fig. 8c).

Next, we examined the joint influence of each of the ten *GR* and *SD* scenarios described above, by running a total of 100 model experiments with both *E1* and *E2* initial conditions. In these simulations, to more realistically represent the historical encroachment process, the observed historical decline in the fire frequency is expressed with a linear increase in fire return period, T_F, from 10 years (in 1861) to 100 years (in 2010) (*F*), consistent with the literature (e.g., [70,96]). The response surfaces for modeled shrub cover in 2010 as a function of changing P_{Mb} (grazing effect) and *SSP* (enhancement in shrub seed dispersal) values are shown in Fig. 9a and b for the *E1* (random) and *E2* (cluster) initial conditions, respectively.

With the *E1* initial vegetation distribution, the final shrub percentage gradually increases with *SSP* and P_{Mb}, from a minimum value of 32.1% to a maximum value of 81.7%. When the *E2* initial vegetation is used (Fig. 7a), the final shrub cover grew from a minimum value of 10.1% representing the minimum values of P_{Mb} and *SSP*, to a maximum value of 78.1%. Note that the minimum values of shrub cover in both surfaces (see circles in Fig. 9a and b) are different than the base simulations (*BØ*) with ~4% shrub cover, as

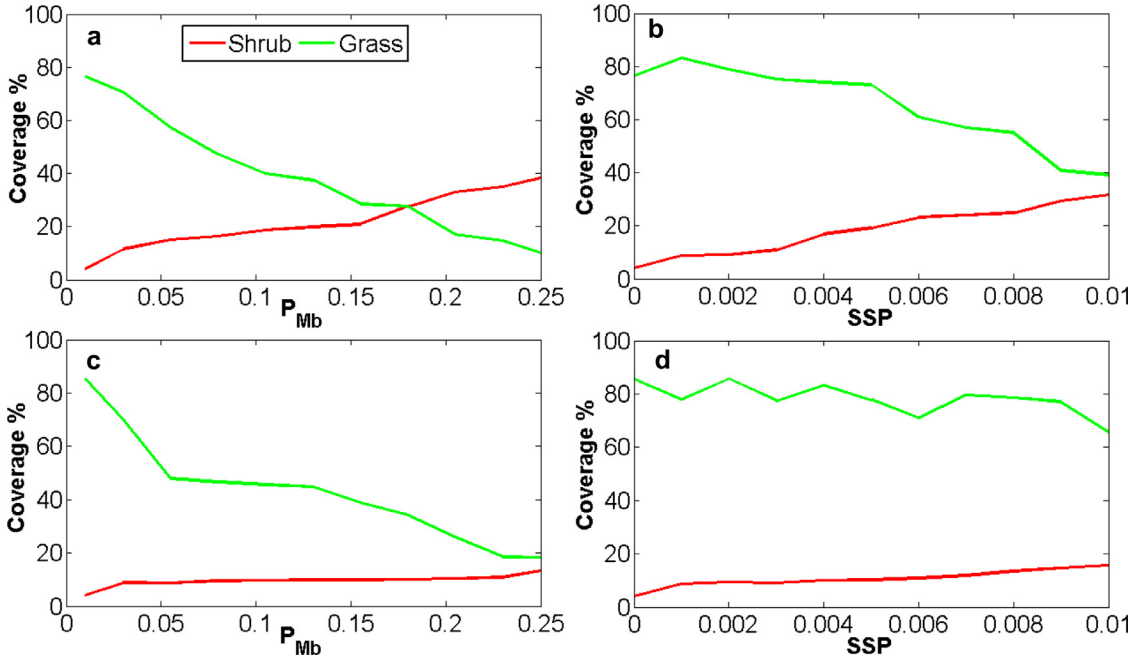

Fig. 8. Final percent coverage of shrub and grass vegetation types with *E1* initial conditions for model sensitivity runs: (a) grazing (*GR*), plotted as a function of mean probability of mortality due to disturbances, P_{Mb}; (b) herbivore influence on seed dispersal (*SD*), illustrated in relation to the spread of seed probability values used, *SSP*. Final percent coverage of shrub and grass vegetation types with *E2* initial conditions for the (c) *GR* and (d) *SD*.

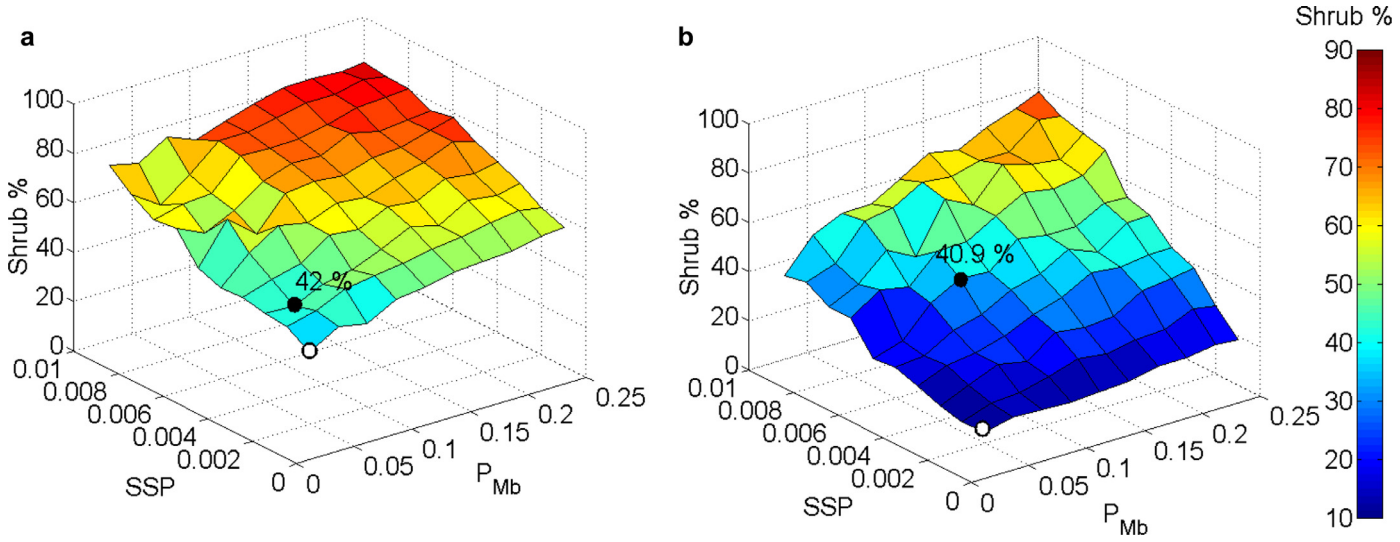

Fig. 9. Final shrub percentage after encroachment for each grazing-seed dispersal cases combination starting from *E1* (a) and from *E2* (b). White-filled circles represent the final shrub percentage values obtained with the minimum values of the background probability of mortality due to disturbances, P_{Mb}, and the spread of seed probability, *SSP*. The black-filled circles provide the "best" reconstruction of encroachment, with shrub cover (%) consistent with the current distribution of shrubs in the study region.

T_F is increased linearly over time throughout the simulations for a more realistic representation of fires, in addition to the use of the minimum values of P_{Mb} and *SSP*. Differences between the two model-response surfaces demonstrate the sensitivity of the model to initial shrub distribution. For a given combination of identical P_{Mb} and *SSP* values for both initial conditions, the *E1* initial condition generally showed a higher shrub cover in the domain than the *E2* initial condition.

The differences between the model response to *E1* and *E2* initial conditions can be largely attributed to the establishment algorithm. When encroachment factors are implemented with individually scattered shrubs across the domain (*E1*) each mature plant actively sends seeds to their neighboring cells. However when shrub clusters dominate the initial condition, plants that are located within the cluster cannot propagate seeds out of the cluster, significantly reducing the seed source as well as the establishment of plants away from the cluster. As a result, ~40% shrub cover is obtained in the *E2* model with a significantly larger seed dispersal effect (*SPP*), and a higher rate of grazing (P_{Mb}).

The proposed fire algorithm for shrubs repeats the random procedure for assessing the fire outcome (burn or survive) for the number of grass cells surrounding the shrub cell (Fig. 4). Because there are limited grass cells within a shrub cluster, shrubs within clusters would survive fires and die only as a function of aging effects. This leads to the development of an older shrub population with the *E2* condition.

For each initial condition we select P_{Mb} and *SSP* values that lead to approximately the observed level of shrub cover, based on the

Table 2
Parameters that give ~40% of shrub cover at the end of the encroachment simulations for the *E1* and *E2* initial conditions.

Cases	Years	T_F [yr]	P_{Mb}[−]	$K_{sg\text{-}G}$ [d^{-1}]	*SSP* [−]
E1	1861–2010	Linearly increasing from 10 to 100	0.05	0.012	0.003
E2			0.1		0.006

NLCD 2006 vegetation map for the study site (Fig. 5a), in both modeled domains (Fig. 9a and b), and report them in Table 2. Because of the slower rates of modeled shrub encroachment in the *E2* domain, parameters that led to the observed shrub cover are twice as large as those found in the model runs with the *E1* domain. The parameter space reported for each initial condition in Table 2 allows us to compare the contribution of each encroachment factor in the model.

4.2.2. Contribution of different encroachment factors on spatial patterns of shrubs

In this section we investigated the modeled spatial outcome of each proposed encroachment factor (*F, GR, SD*) individually, two-factor combinations, and finally all 3 factors combined using the parameters reported in Table 2. Combination of all three factors for *E1* and *E2* initial conditions give the black-filled circles in Fig. 9a and b. Model outputs are reported in Figs. 10 and 11 for *E1* and *E2* initial conditions, respectively. *BØ* output is presented for comparison of natural conditions without human-introduced herbivores and with more frequent fires representing the historical grassland fire regime. When encroachment factors are not introduced 4% shrub cover remains stable in the model during the 150-year encroachment period as shown in the baseline simulations (see *BØ* in Figs. 10 and 11). In *E1* (Fig. 10), some shrub clusters evolved from randomly distributed plants while other individual shrubs died with no net change in % shrub cover over the 150-year long simulation.

With the *E1* initial condition, reduction in fire frequency (*F*) provides the largest increase in shrub (*SH*) cover among all the encroachment factors considered, followed by biomass removal and mortality due to grazing (*GR*) (Fig. 10). Loss of grass (*G*) in the *F* simulation is a result of shrubs becoming more competitive, as they mature and actively disperse seeds with less frequent fires. *SD* also has a pronounced effect on the growth of shrub clusters by providing an increased probability of space filling by shrubs. Factors *F* and *GR* combined only adds ~5% more shrubs in the modeled domain, while it has a marked influence on the decline of grass coverage by more than 20%, compared to the effect of *F* only. This model finding is consistent with experimental results of Gosz and Gosz [43], who suggest grazing as a major cause of loss of black grama (*B. eriopoda*). Combination of all factors (*F-GR-SD*) leads to the final shrub cover of 42%, adding 8% more shrubs to the case of *F-GR*, while grass covers drops by about 7%.

In the case of *E2* initial condition (Fig. 11), the model response to individual encroachment factors (*F, GR, SD*) is relatively muted. Among the individual factors, *SD* causes the largest increase in shrub cover from 4.23% to 10.79%. Among the two-factor combination runs, *GR-SD* combined leads to the largest increase in shrub (+14%) and decrease in grass (−29%) cover from the baseline simulation. This is anticipated in this model as grazing actively removes grass cells, while increase in the probability of shrub establishment due to *SSP* fills empty cells. With the *E2* initial condition the model shows significant response only when all three encroachment factors are incorporated. In the *F-GR-SD* scenario shrub cover doubles and grass cover reduces by half compared to the *GR-SD* simulation. In both *E1* and *E2* scenarios increase in shrub cover in the *F-GR-SD* simulations compared to the *GR-SD* simulations can be attributed to the maturing of shrubs to active age of seed dispersal (i.e.,18 years of age) as fire return period grows beyond 10 years. *SD* effect was more pronounced in the *E2* simulation (*F-GR-SD*) compared to

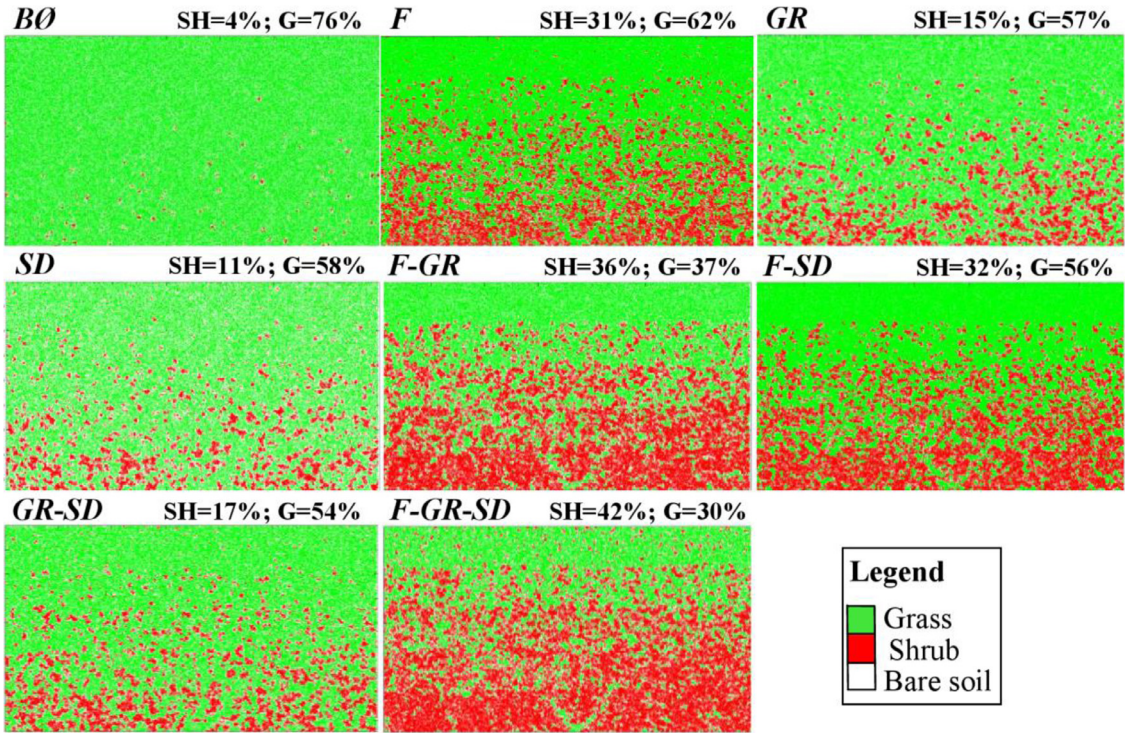

Fig. 10. Final vegetation distribution maps for the implementation of different combinations of encroachment factors (*F*: fires, *GR*: grazing, *SD*: seed dispersal by grazers) for the *E1* initial condition. *BØ* is the baseline simulation (i.e., without encroachment factors). Percent cover of shrub (*SH*) and grass (*G*) are reported for each map.

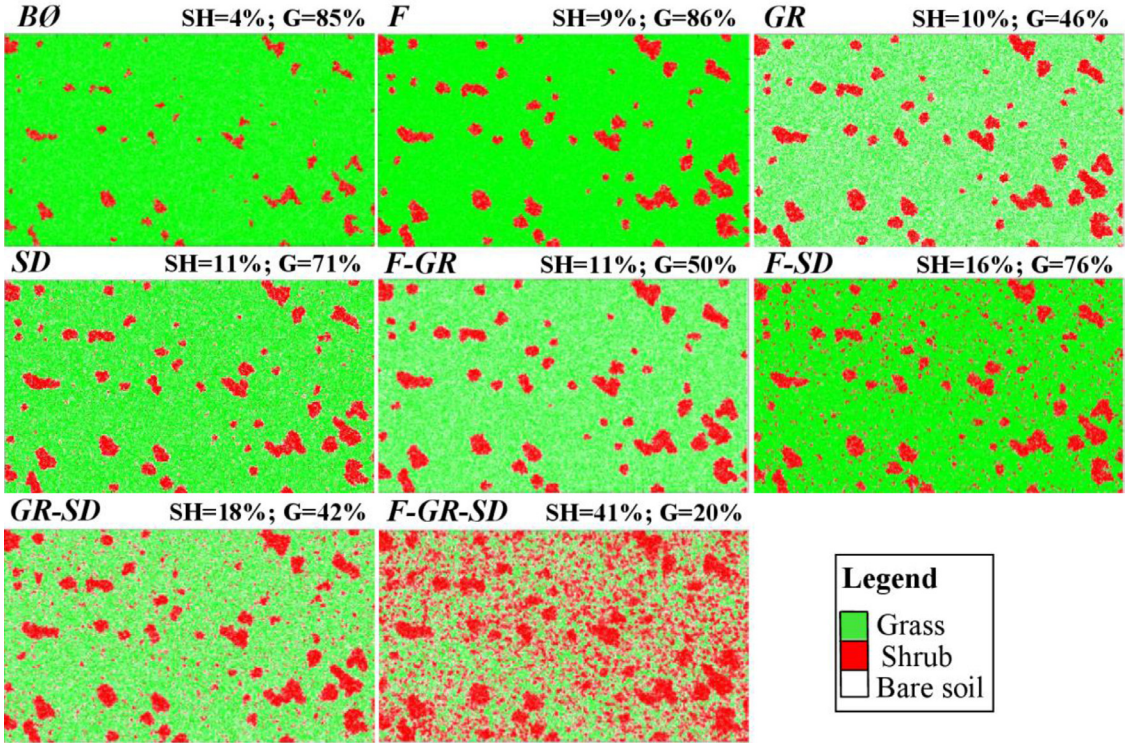

Fig. 11. Final vegetation distribution maps for the implementation of different combinations of encroachment factors (*F*: fires, *GR*: grazing, *SD*: seed dispersal by grazers) for the *E2* initial condition. *BØ* is the baseline simulation (i.e., without encroachment factors). Percent cover of shrub (*SH*) and grass (*G*) are reported for each map.

E1. This is because in *E2* shrub propagation is largely attributed to increase in the spread of seed probability (*SSP*) as individual shrubs inside the clusters cannot disperse seeds to empty cells out of the cluster. Therefore as fire return interval increases, shrubs that establish as a result of the *SD* effect mature and begin dispersing seeds and hence enhance shrub cover in the domain.

4.2.3. The role of climate variability on encroachment

In the simulations reported above a single stationary realization of the weather generator was run, and used consistently in all vegetation simulation experiments. This approach neglects the stochastic nature of the climate and does not allow for the analysis of the role of observed historical droughts in the last 150 years. In order to investigate the stochastic nature of the local climate on simulated vegetation fields, we ran CATGraSS with an ensemble of 50 realizations using all three factors of encroachment (*F-GR-SD)* on an *E1* domain. In each run different random seeds are used to generate different weather forcings while the overall statistical properties of the climate were kept constant.

In addition to addressing the stochastic nature of the climate, we also investigated the influence of the 1950 s drought (Fig. 6) as well as observed variations in the historical climate in the SNWR using the daily time series of temperature and precipitation measured at SCS from 1893 to 2010. The drought in the 1950 s provides a natural perturbation experiment to shrub encroachment.

In Fig. 12 we plot the median, and the 10th and the 90th percentiles of simulated shrub and grass cover trajectories from the stochastic CATGraSS simulations; as well as shrub and grass cover for the simulation driven by the historical daily weather data in SCS. It is important to point out that SCS is located only 35 km south of the study site, however it represents the characteristics of the central New Mexico climate.

The median trajectory highlights an increase of shrubs from 4% in 1860 to 42.26% in 2010, and loss of grass from 80% in 1860 to 29% in 2010, consistent with Fig. 10 (*F-GR-SD*). Stochastic climate has a small impact on the final shrub cover in the domain in 2010, while higher variability in grass cover reflects its sensitivity to inter-annual fluctuations in precipitation. The observed climate starts with approximately a decade-long wet period, followed by average conditions that continue until the beginning of drought conditions by the mid 1940 s (Fig. 6). The simulation forced with historical data shows shrub encroachment close to the 90th percentile line of the stochastic simulations before drought. Between 1940 and 1960, shrub cover drops from ~27% in 1941 to ~16% in 1956 (lowest shrub cover after 1940), while grass cover continuously declines from ~47% to ~25%. Shrub cover increases again as rainfall returns to average after 1960. During the drought period 1940–1960, shrub cover drops under the 10th percentile of the shrub cover trajectory obtained through the stochastic ensemble;

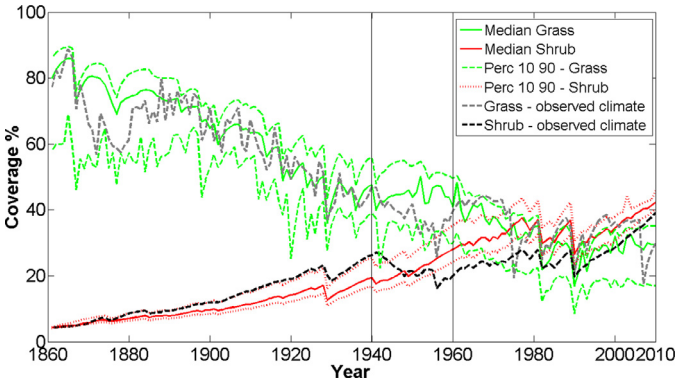

Fig. 12. Grass (green line) and shrub (red line) coverage over time for 50 stationary climate runs (median, 10th percentile and 90th percentile), compared with grass (dashed gray line) and shrub (dashed black line) coverage obtained by forcing the model with the observed climate in Socorro (factors combination *F-GR-SD, E1*). (For interpretation of the references to color in this figure legend, the reader is referred to the web version of this article.)

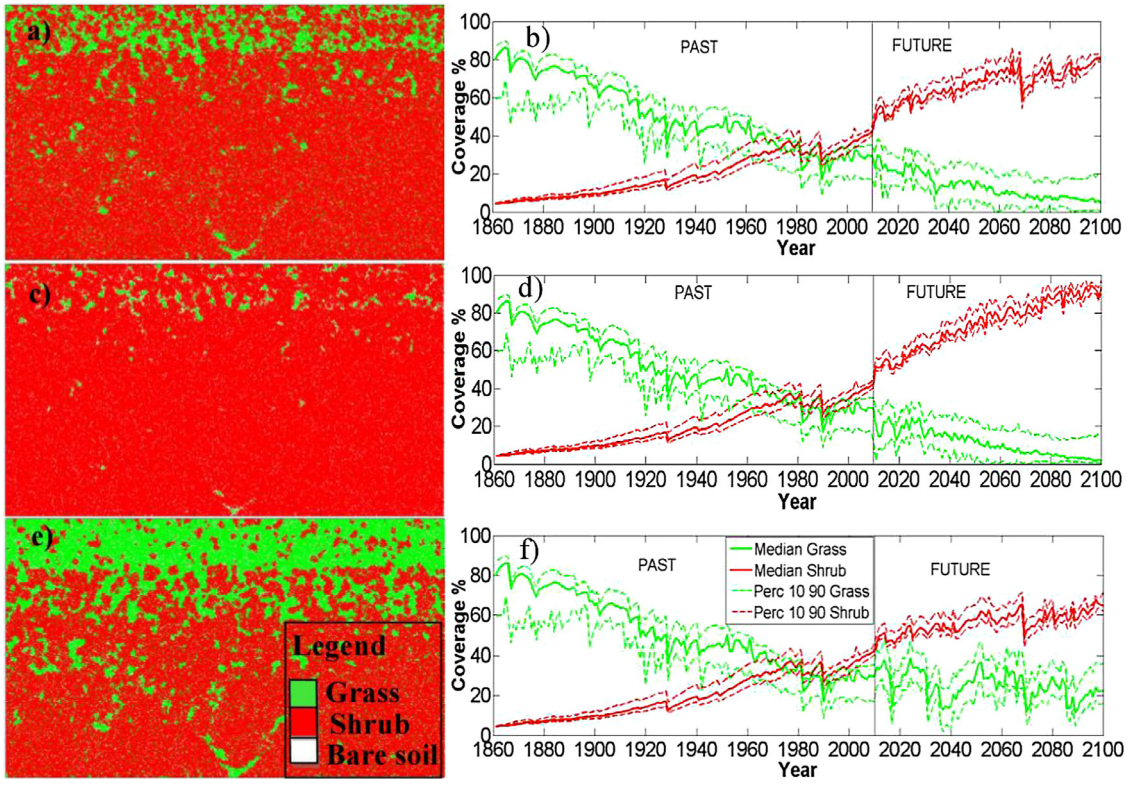

Fig. 13. Modeled impact of climate (historical and future) on shrub encroachment. Left panels show vegetation maps at year 2100 and right panels plot time series of the median, the 10th and the 90th percentiles of annual shrub and grass cover percentages obtained from 50 ensemble member simulations between 1860 and 2100. Scenarios plotted from top to bottom are: *BL*, *CGF*, and *CNGF* as described in 4.2.4.

this could occur because precipitation observed in this period was lower than the 10th percentile of the stochastic ensemble of precipitation provided by AWE-GEN, denoting a strong relationship between rainfall forcings and shrub dynamics. The result of the simulation driven by the historical data provided by SCS is consistent with Stewart et al. [88] who argued that droughts slow down rather than promote shrub encroachment. Interestingly, despite the differences in the stochastic sequences of rainfall events and a sustained drought in the historical simulations, shrub cover trajectories (historical and ensemble median) evolve nearly in parallel especially after the 1950 s drought reaching, at the end of the simulation period, almost the same vegetation coverage. This may suggest a strong control of fire and of the initial vegetation cover used in the beginning of the simulations.

4.3. Climate change impacts on shrub encroachment

Our model clearly responds to drier conditions during the 1940-1960 drought period (Fig. 12). This result naturally leads to the following questions: (1) how will climate change impact shrub encroachment in central New Mexico in the future? (2) Can removal of grazing and restoring fire frequency to pre-grazed conditions reduce shrub encroachment in the future? To investigate these questions, CATGraSS is used to simulate vegetation dynamics in the 21st century starting with the simulated vegetation distribution in 2010 for the *F-GR-SD* scenario presented in Figs. 10 and 12.

Three climate scenarios are developed: (1) a baseline scenario where climate is kept stationary without any future change while grazing and low fire frequency continued (*BL* scenario); (2) a future climate change scenario with continued grazing and low fire frequency (*CGF* scenario); (3) a future climate change scenario in the absence of grazing with natural fire frequency (*CNGF* scenario). An ensemble of 50 simulations driven by AWE-GEN is conducted for each scenario. When grazing is removed all model parameters are set to baseline spin-up conditions discussed earlier.

Fig. 13 maps vegetation distribution in 2100 (left panels) in one of the ensemble members, and the time series of the median, the 10th and the 90th percentiles of annual shrub and grass cover percentages obtained from 50 ensemble member simulations between 1860 and 2100 (right panels). Fig. 13 presents *BL*, *CGF*, and *CNGF* scenarios in respective order from top to bottom. Percentiles of cover are preferred here to illustrate the uncertainty in the vegetation cover as a result of stochastic climate. The results of the *BL* scenario clearly shows that shrub encroachment in the region may continue with continuing grazing without any future climate change, doubling the shrub cover by the end of 2100 (Fig. 13a and b). In the *CGF* scenario a drier climate brings 13% more shrubs in the model, predicting a faster shrub encroachment in the future with grazing compared to the *BL* scenario (Fig. 13c and d). In the *CNGF* scenario encroachment continues at a much reduced rate and the simulation ends with much lower median shrub cover of ~64% in 2100 (Fig. 13e and f) compared to *CGF* that ended with ~90% shrub cover (Fig. 13c and d). Absence of grazing also leads to higher inter-annual variability in grass cover. These results support the conclusions of Ravi and D'Odorico [79], who suggested that removal of grazing and restoring historic fire frequencies may slow down shrub encroachment.

CATGraSS simulations suggest that climate change will favor shrub encroachment even when grazing is removed. This behavior can be ecohydrologically explained by plotting the probability of exceedance of water stress (WS_X) for shrub and grass vegetation for the historical (1860–2010) and the future (2011–2100) modeled periods (Fig. 14). WS_X is calculated at the end of each growing season, and used to calculate annual probabilities of plant establishment and mortality due to drought stress as described earlier (see also [98]). In each modeled year the median value

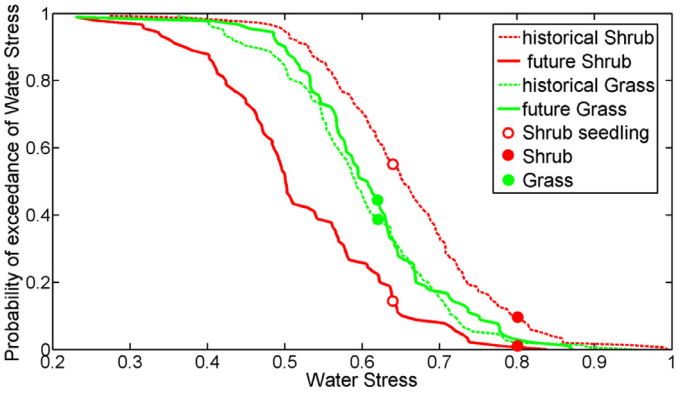

Fig. 14. Exceedance probabilities of modeled annual plant water stress (WS_X) and calibrated drought resistance thresholds (circles) plotted for shrub and grass vegetation types for historical and future climate change simulations.

of spatially averaged WS_X for shrub and grass is selected from the 50 ensemble simulations. Fig. 14 shows a marked decrease in shrub *WS* under climate change, as the *WS* distribution shifts to lower values, while grass experiences a very slight increase in *WS*. Filled circles in Fig. 14 represent the calibrated drought resistance thresholds (θ_X) for shrub, grass, and shrub seedlings (open circle) (Table 1). When WS_X exceeds θ_X, probability of plant mortality increases. Therefore calculating the probability of exceedance of a given θ_X, $P(WS_X \geq \theta_X)$ would be a relevant measure to quantify the impact of climate change on plant mortality. $P(WS_X \geq \theta_X)$ for mature shrubs decreases from 0.1 in the historical period to 0.022 in the future period, while for shrub seedlings $P(WS_X \geq \theta_X)$ decreases from 0.55 in the historical period to 0.15 in the future period. In contrast, $P(WS_X \geq \theta_X)$ for grass increases from 0.38 in the historical period to 0.45 in the future period.

Creosotebush, the dominant shrub in central New Mexico, is drought tolerant as it has deeper roots and resistant physiology [25,49,81], while black grama grass is less tolerant to short droughts, but can recover rapidly when soil water is available [8,20]. Our model simulations are consistent with Allen and Breshears [2] and van Auken [93] who suggest that climate change could exacerbate future WPE. In a recent study Gherardi and Sala [40] examined the impact of climate change on shrub and grass vegetation by increasing the inter-annual variability of rainfall in a rainfall manipulation experiment conducted at the Jornada Basin Long Term Ecological Research (LTER) site, New Mexico, USA. Dry years had a larger impact on loss of grass productivity than productivity gain in wet years, resulting in net loss of grass productivity over the 6-year study period. Shrub productivity increased with growing rainfall variability. Gherardi and Sala [40] attributed the increase in productivity of shrubs and decrease in productivity of grasses to differences in their rooting depths.

5. Conclusions

Arid and semiarid grasslands of southwestern North America have changed dramatically over the last 150 years as a result of woody plant encroachment (WPE). WPE has important implications in the management of water and land resources of the impacted regions. Therefore, understanding and realistically representing the past and future ecohydrologic dynamics of WPE is of paramount importance. Many have argued that domestic herbivores, reduced fire frequency and climate change are primary causes of WPE in this region. Relatively simple algorithms for grazing, grassland fires, and seed dispersal effects of grazing herbivores are proposed and incorporated in the *Cellular Automaton Tree-Grass-Shrub Simulator* (CATGraSS), which is implemented in a small area (7.3 km^2) in central New Mexico where shrub encroachment into grassland is active with ~40% shrub cover currently. Our model experiments included three phases: long-term spin-up, historical encroachment, and future climate change simulations. Our major findings are summarized as:

(1) The model is highly sensitive to the distribution of pre-encroachment shrub cover as model initial condition. When a small areal percentage (i.e., 4%) of shrubs is randomly distributed that gradually decreases moving northward (*E1* scenario) as a model initial condition (*E1*), encroachment factors more actively lead to shrub propagation. However, when shrubs are grouped in clusters as a model initial condition (*E2*), the model response to encroachment factors is muted. This response is attributed to the fact that shrubs within a cluster do not send seeds outside the cluster unless they are located on the cluster boundary. This model response is compensated for by selecting higher model parameter values in *E2* than *E1* simulations to obtain roughly the same amount of shrub cover in both models.

(2) Under starting conditions where shrub cover gradually decreases moving northward (*E1* scenario), the model simulates historical shrub encroachment, reproducing an increase in shrub cover from 2% to 42%. The simulations indicate that the most influential factors driving shrub encroachment under these conditions are reduced fire frequency, and increased grazing intensity, as proposed by van Auken [92,93]. These simulations also indicated that shrub encroachment is not facilitated by drought periods. Under starting conditions where shrubs are clustered (*E2* scenario), the most influential factor limiting shrub encroachment is seed dispersal by animals under reduced fire frequency and increased grazing.

(3) CATGraSS predicted loss of shrub and grass cover during the 1950 s drought. Between 1940 and 1960 shrub cover drops from ~27% in 1941 to ~16% in 1956, while grass cover continuously declines from 47% to 25%. Shrub cover begins to increase again as rainfall returns to average after 1960. Grass cover on the other hand first shows some recovery, followed by decline. The result of the simulation driven by the historical data provided by a nearby weather station is consistent with Stewart et al. [88] who argued that droughts slow down rather than promote shrub encroachment.

(4) Trajectories of modeled shrub and grass cover driven by a stochastic weather generator suggest a relatively low (high) sensitivity of shrub (grass) cover to climate variability over the 150-year long encroachment simulations. While higher variability in grass cover reflects the sensitivity of grass to inter-annual fluctuations in precipitation, consistence between the trajectories of modeled shrub cover driven by historic and stochastic climate suggest a strong control of fire and shrub spatial patterns on shrub response. These results suggest a highly predictable system sensitive to initial conditions.

(5) In the future simulations, while climate change is found to amplify shrub encroachment (~13% more shrub cover by 2100), grazing is found to be the dominant factor that leads to shrub encroachment. When grazing is removed and the fire frequency is set to pre-grazing conditions, encroachment continues with a reduced rate under future climate change. Existing, widespread seed sources from mature shrub plants can be an explanation of continuing encroachment without grazing. However, the model also predicts lower shrub water stress under climate change which reduces shrub mortality rate and improves shrub encroachment. Predicted shrub encroachment with climate change is consistent with recent literature.

Limited mechanistic understanding of shrub encroachment and uncertainties in the representation of ecohydrological factors to reproduce this phenomenon hamper the development and use of numerical models [48,55]. In addition, simulations can provide similar "acceptable" patterns of grass and shrub abundances denoting the presence of equifinality in models [11]. The coupled ecohydrological cellular automaton modeling approach presented here provides a "tool box" for testing hypothesis about WPE. Changes in fire frequency, seed dispersal caused by animals, and grazing have been implemented in the model separately, but these variables likely interact with each other and additional drivers to promote shrub encroachment. Therefore, future efforts could enhance the model by connecting these three variables with other drivers, to determine how fire, grazing and climate change will interact to drive shrub encroachment and vegetation dynamics under global environmental change. Another future improvement of the cellular automata model will be the introduction of a geomorphic component that takes into account erosion and transport of sediment by wind and water and sediment-vegetation interactions such that the development of islands of fertility can be simulated and examined in this model. Lack of such coupled eco-hydro-geomorphic processes is a critical limitation of the current model.

Acknowledgments

We thank the reviewers and handling editor for many valuable comments that greatly improved the manuscript. We acknowledge Conrad J. Bahre, M.L. Shelton, the Journal of Biogeography and the Wiley library that permitted us to use the pictures in Fig. 1d, e. Reference: *Bahre, C.J. and Shelton, M.L. (1993). "Historic vegetation change, mesquite increases, and climate in southeastern Arizona". Journal of Biogeography, 20, 489–504, copyright © 1993, published by Wiley.* Istanbulluoglu acknowledges NSF for financial support provided through grant: NSF-ACI 1148305. Collins was supported by grants from NSF to the University of New Mexico for Long-term Ecological Research.

References

[1] Accatino F, De Michele C, Vezzoli R, Donzelli D, Scholes RJ. Tree-grass co-existence in savanna: interactions of rain and fire. J Theor Biol 2010;267:235–42.
[2] Allen CD, Breshears DD. Drought-induced shift of a forest-woodland ecotone: rapid landscape response to climate variation. Proc Natl Acad Sci USA 1998;95:14839–42.December 1998.
[3] Allen, C.D., Betancourt, J., Swetnam, T. (2002). Range expansion of woody plants on the Colorado Plateau. In: Grahame, J.D., Sisk, T.D. editors. http://www.cpluhna.nau.ed/.
[4] Allen RG, Trezza R, Tasumi M. Analytical integrated functions for daily solar radiation on slopes. Agric For Meteorol 2006;139:55–73.
[5] Archer S. Woodly plant encroachment into southwestern grasslands and savannas: rates, patterns and proximate causes. Ecological implications of livestock herbivor in the west. Denver: Soc Range Manage; 1994. p. 13–69.
[6] Báez S, Collins SL, Lightfoot D, et al. Effects of rodent removal on community dynamics in desert grassland and shrubland vegetation. Ecology 2006;87:2746–54.
[7] Báez S, Collins SL. Shrub invasion decreases diversity and alters community stability in Northern Chihuahuan Desert plant communities. PLoS ONE 2008;3:e2332. http://dx.doi.org/10.1371/journal.pone.0002332.
[8] Báez S, Collins SL, Pockman WT, Johnson JE, Small EE. Effects of experimental rainfall manipulations on Chihuahuan Desert grassland and shrubland plant communities. Oecologia 2013;172:1117–27.
[9] Bahre CJ, Shelton ML. Historic vegetation change, mesquite increases, and climate in southeastern Arizona. J Biogeogr 1993;20:489–504.
[10] Bestelmeyer BT, Duniway MC, James DK, Burkett LM, Havstad KM. A test of critical thresholds and their indicators in a desertification-prone ecosystem: more resilience than we thought. Ecol Lett 2013;16:339–45.
[11] Beven KJ. Prophecy, reality and uncertainty in distributed hydrological modeling. Adv Water Resour 1993;16:41–51.
[12] Bhark EW, Small EE. Association between plant canopies and the spatial patterns of infiltration in shrubland and grassland of the Chihuahuan desert, New Mexico. Ecosystems 2003;6:185–96.
[13] Bond WJ, Woodward FI, Midgley GF. The global distribution of ecosystems in a world without fire. New Phytol 2005;165:525–37. http://dx.doi.org/10.3410/f.1033415.375868.
[14] Bond WJ, Midgley GF. Carbon dioxide and the uneasy interactions of trees and savannah grasses. Phil Trans Roy Soc B 2012;367:601–12.
[15] Bowers JE, Webb RH, Rondeau RJ. Longevity, recruitment and mortality of desert plants in Grand Canyon, USA. J Veg Sci 1995;6:551–64.
[16] Browning DM, Archer SR, Asner GP, McClaran MP, Wessman CA. Woody Plants in grasslands: post-encroachment stand dynamics. Ecol Appl 2008;18(4):928–44.
[17] Browning DM, Franklin J, Archer SR, Gillan JK, Phillips D. Spatial patterns of grassland-shrubland state transitions: a 74-year record on grazed and protected areas. Ecol Appl 2014;24:1421–33.
[18] Brunelle A, Minckley TA, Delgadillo J, Blissett S. A long-term perspective on woody plant encroachment in the desert southwest, New Mexico, USA. J Veg Sci 2013;25:829–38.
[19] Buffington LC, Herbel H. Vegetational Changes on a semidesert grassland range from 1858 to 1963. Ecol Monogr 1965;35(2):139–64.
[20] Burgess TL, McClaran MP, Van Devender TR. Desert grassland, mixed shrub savanna, shrub steppe or semidesert scrub. The dilema of coexisting forms. The desert grassland. Tuscon, Arizona, USA: University of Arizona Press; 1995. p. 31–67.
[21] Burkhardt JW, Tisdale EW. Causes of juniper invasion in southwestern Idaho. Ecology 1976;57:472–84.
[22] Burton A, Fowler HJ, Blenkinsop S, Kilsby CG. Downscalingtransient climate change using a Neyman-Scott Rectangular Pulses stochastic rainfall model. J Hydrol 2010;381:18–32. http://dx.doi.org/10.1016/j.jhydrol.2009.10.031.
[23] Caracciolo D, Noto LV, Istanbulluoglu E, Fatchi S, Zhou X. Climate change and Ecotone boundaries: insights from a cellular automata ecohydrology model in a Mediterranean catchment with topography controlled vegetation patterns. Adv Water Resour 2014;73:159–75.
[24] Casagrandi R, Rinaldi S. A minimal model for forest fire regimes. Am Nat 1999;153:5.
[25] Casper BB, Jackson RB. Plant competition below ground. Annu Rev Ecol Syst 1997;28:545–70.
[26] Charley JL, West NE. Plant-induced soil chemical patterns in some shrub-dominated semi-desert ecosystems of Utah. J Ecol 1975;63(3):945–63. http://dx.doi.org/10.2307/2258613.
[27] Chew RM, Chew AE. The primary productivity of a desert-shrub (Larrea tridentata) community. Ecol Monogr 1965;35(4):355–75.
[28] Christensen JH, Konikicharla KK, Stoker TF, Qin D, Platter GK, Tignor M, Allen SK, Boschung J, Navels A, Xia Y, Bex V, Midgley PM. Climate phenomena and their relevance for future regional climate change. Climate Change 2013: The Physical Science Basis, Contribution of Working Group I to the Fifth Assessment Report of the Intergovernmental Panel on Climate Change. Cambridge, UK: Cambridge University Press; 2013. p. 1217–308.
[29] Collins SL, Xia Y. Long-term dynamics and hot spots of change in a desert grassland plant community. Am Nat 2015;185(2):E30–43. http://dx.doi.org/10.1086/679315.
[30] Cook BI, Ault TR, Smerdon JE. Unprecedented 21st century drought risk in the American Southwest and Central Plains. Sci Adv 2015;1:e1400082.
[31] Coop JD, Givnish TJ. Spatial and temporal patterns of recent forest encroachment in montane grasslands of the Valles Caldera, New Mexico, USA. J Biogeogr 2007;34:914–27.
[32] D'Odorico P, Laio F, Ridolfi L. A probabilistic analysis of fire-induced tree-grass coexistence in savannas. Am Nat 2006;167(3):E79–87.
[33] D'Odorico P, Fuentes JD, Pockman WT, Collins SL, He Y, Medeiros JS, et al. Positive feedback between microclimate and shrub encroachment in the northern Chihuahuan desert. Ecosphere 2010;1(6):art.17 http://dx.doi.org/10.1890/ES10-00073.1.
[34] D'Odorico P, Okin GS, Bestelmeyer BT. A synthetic review of feedbacks and drivers of shrub encroachment in arid grasslands. Ecohydrology 2012;5:520–30.
[35] Doerr SH, Shakesby RA, Walsh RPD. Soil water repellency: its causes, characteristics and hydro-geomorphological significance. Earth Sci Rev 2000;51:33–65.
[36] Eldridge DJ, Bowker MA, Maestre FT, Roger E, Reynolds JR, Whitford WG. Impacts of shrub encroachment on ecosystem structure and functioning: towards a global synthesis. Ecol Lett 2011;14:709–22.
[37] Fatichi S, Ivanov VY, Caporali E. Simulation of future climate scenarios with a weather generator. Adv Water Resour 2011;34(4):448–67.
[38] Fatichi S, Ivanov VY, Caporali E. Assessment of a stochastic downscaling methodology in generating an ensemble of hourly future climate time series. Clim Dyn 2013;40(7--8):1841–61.
[39] Frost PGH, Robertson F, Walker BK. The ecological effect of fire in savannas. Determinants of Tropical Savannas. Miami: ICSU Press; 1987. p. 93–140.
[40] Gherardi LA, Sala OE. Enhanced interannual precipitation variability increases plant functional diversity that in turn ameliorates negative impact on productivity. Ecol Lett 2015;18(12):1293–300. http://dx.doi.org/10.1111/ele.12523.
[41] Gherardi LA, Sala OE. Enhanced precipitation variability decreases grass- and increases shrub-productivity. PNAS 2015;112(41):12735–40. http://dx.doi.org/10.1073/PNAS2015.
[42] Gosz JR, Moore DI, Shore GA, Grover HD, Rison W, Rison C. Lightning estimates of precipitation location and quantity on the Sevilleta LTER, New Mexico. Ecol Appl 1995;5:1141–50.
[43] Gosz RJ, Gosz JR. Species interactions on the biome transition zone in New Mexico: response of blue grama (Bouteloua gracilis) and black grama (Bouteloua eriopoda) to fire and herbivory. J Arid Environ 1996;34:101–114.

[44] Grover HD, Musick HB. Shrubland encroachment in Southern New Mexico, U.S.A.: an analysis of desertification processes in the American Southwest. Clim Chang 1990;17:305–30.
[45] Gutiérrez-Jurado HA, Vivoni ER, Harrison JBJ, Guan H. Ecohydrology of root zone water fluxes and soil development in complex semiarid rangelands. Hydrol Process 2006;20:3289–316.
[46] Gutzler DS, Robbins TO. Climate variability and projected change in the western United States: regional downscaling and drought statistics. Clim Dyn 2011;37:835–49.
[47] He Y, D'Odorico P, De Wekker SFJ, Fuentes JD, Litvak M. On the impact of shrub encroachment on microclimate conditions in the northern Chihuahuan desert. J Geophys Res 2010;115:D221120. http://dx.doi.org/10.1029/2009JD013529.
[48] He Y, D'Odorico P, De Wekker SFJ. The role of vegetation-microclimate feedback in promoting shrub encroachment in the northern Chihuahuan desert. Glob Chang Biol 2015;21(6):2141–54. http://dx.doi.org/10.1111/gcb.12856.
[49] Herbel CH, Ares FN, Wright RA. Drought effects on a semidesert grassland range. Ecology 1972;53:1084–93.
[50] IPCC. Climate change 2007: The Physical Science Basis. Contribution of Working Group I to the Fourth Assessment Report of the Intergovernmental Panel on Climate Change. Cambridge and New York, NY: Cambridge University Press; 2007.
[51] Istanbulluoglu E, Bras RL. On the dynamics of soil moisture, vegetation, and erosion: implications of climate variability and change. Water Resour Res 2006;42:W06418 2006. http://dx.doi.org/10.1029/2005WR004113.
[52] Ivanov VY, Bras RL, Curtis DC. A weather generator for hydrological, ecological, and agricultural applications. Water Resour Res 2007;43:364 W10,40. http://dx.doi.org/10.1029/2006WR005.
[53] Jeltsch F, Milton SJ, Dean WRJ, van Rooyen N. Tree spacing and coexistence in semi-arid savannas. J Ecol 1996;84:583–95.
[54] Jeltsch F, Milton SJ, Dean WRJ, van Rooyen N, Moloney KA. Modelling the impact of small-scale heterogeneities on tree-grass coexistence in semi-arid savannas. J Ecol 1998;86(5):780–93.
[55] Knapp AK, Briggs JM, Collins SL, Archer SR, Bret-Harte MS, Ewers BE, et al. Shrub encroachment in North American grasslands: shifts in growth form dominance rapidly alters control of ecosystem carbon inputs. Glob Chang Biol 2008;14:615–23.
[56] Knipe D, Herbel CH. Germination and growth of some semidesert grassland species treated with aqueous extract from creosotebush. Ecology 1966;47(5):775–81.
[57] Kurc SA, Small EE. Dynamics of evapotranspiration in semiarid grassland and shrubland during the summer monsoon season, central New Mexico. Water Resour Res 2004;40:W09305. http://dx.doi.org/10.1029/2004WR003068.
[58] Laio F, Porporato A, Ridolfi L, Rodriguez-Iturbe I. Plants in water controlled ecosystems: active role in hydrologic processes and response to water stress II. Probabilistic soil moisture dynamics. Adv Water Resour 2001;24:707–23.
[59] Laliberte AS, Rango A, Havstad KM, Paris JF, Beck RF, McNeely R, et al. Object-oriented image analysis for mapping shrub encroachment from 1937 to 2003 in southern New Mexico. Remote Sens Environ 2004;93:198–210 2004.
[60] Liu F, Archer SR, Gelwick F, Bai E, Boutton TW, Wu XB. Woody plant encroachment into grasslands: spatial patterns of functional group distribution and community development. PLoS One. 2013 Dec 18 2013;8(12):e84364.
[61] McGlynn IO, Okin GS. Characterization of shrub distribution using high spatial resolution remote sensing: ecosystem implications for a former Chihuahuan Desert grassland. Remote Sens Environ 2006;101:554–66 2006.
[62] Meehl GA, Stocker TF, Collins WD, Friedlingstein P, Gaye AT, Gregory JM, Solomon S, Qin D, Manning M, Chen Z, Marquis M, Averyt KB, Tignor M, Miller HL, et al. Global Climate Projections Climate Change 2007: The Physical Science Basis, Contribution of Working Group I to the Fourth Assessment Report of the Intergovernmental Panel on Climate Change. Cambridge, United Kingdom and New York, NY, USA: Cambridge University Press; 2007.
[63] Miller RF, Bates JD, Svejcar TJ, Pierson FB, Eddleman LE. Biology, ecology, and management of western juniper. Technical bulletin 152. Oregon State University, Agricultural Experiment Station; 2005. p. 77.
[64] Milne BT, Moore DI, Betancourt JL, David Greenland Douglas, Goodin G, Raymond C, Smith, et al. Multidecadal drought cycles in South-Central New-Mexico: Patterns and Consequences Climate Variability and Ecosystem Response at Long-Term Ecological Research Sites; 2003.
[65] Montaldo N, Rondena R, Albertson JD, Mancini M. Parsimonious modeling of vegetation dynamics for ecohydrologic studies of water-limited ecosystems. Water Resour Res 2005;41:W10416. http://dx.doi.org/10.1029/2005WR004094.
[66] Okin GS, Gillette DA. Distribution of vegetation in wind-dominated landscapes: implications for wind erosion modeling and landscape processes. J Geophys Res 2001;106(9):9673–83. http://dx.doi.org/10.1029/2001JD900052.
[67] Okin GS, Parsons AJ, Wainwright J, Herrick JE, Bestelmeyer BT, Peters DPC, et al. Do changes in connectivity explain desertification? Bioscience 2009;59:237–44.
[68] Okin GS, D'Odorico P, Archer SR. Impacts of feedbacks on Chihuahuan Desert grasslands: transience and metastability. J Geophys Res 2009;114:G01004.
[69] Okin GS, Moreno-de lAS, Heras M, Saco PM, Throop HL, Vivoni ER, et al. Connectivity in dryland landscapes: shifting concepts of spatial interactions. Front Ecol Environ 2015;13:20–7.
[70] Parmenter RR. Long-term effects of summer fire on desert grassland plant demographics in New Mexico. Rangel Ecol Manag 2008;61:156–68.
[71] Peters DPC. Plant species dominance at a grassland-shrubland ecotone: an individual-based gap dynamics model of herbaceous and woody species. Ecol Model 2002;152:5–32.
[72] Peters DPC, Pielke RA, Bestelmeyer BT, Allen CD, Munson-McGee S, Havstad KM. Cross-scale interactions, non-linearities, and forecasting catastrophic events. Proc Natl Acad Sci 2004;101:15130–5.
[73] Peters DCP, Yao J. Long-term experimental loss of foundation species: consequences for dynamics at ecotones across heterogeneous landscapes. Ecosphere 2012;3(3):27 http://dx.doi.org/10.1890/ES11-00273.1.
[74] Petrie MD, Collins SL, Gutzler D, Moore DI. Regional trends and local variability in monsoon precipitation in the northern Chihuahuan Desert, USA. J Arid Environ 2014;103:63–70.
[75] Petrie MD, Collins SL, Ford PL, Swann AM, Litvak M. Grassland to shrubland state transitions enhance carbon sequestration in the northern Chihuahuan Desert. Glob Chang Biol 2015;21:1226–35. http://dx.doi.org/10.1111/gcb.12743.
[76] Porporato A, Laio F, Ridolfi L, Rodriguez-Iturbe I. Plants in water-controlled ecosystems: active role in hydrological processes and response to water stress, III, vegetation water stress. Adv Water Resour 2001;24:725–44.
[77] Ratajczak Z, Nippert JB, Collins SL. Woody encroachment decreases diversity across North American grasslands and savannas. Ecology 2012;93:697–703.
[78] Ravi S, D'Odorico P, Zobeck TM, et al. Feedbacks between fires and wind erosion in heterogeneous arid lands. J Geophys Res 2007;112:G04007. http://dx.doi.org/10.1029/2007JG000474.
[79] Ravi S, D'Odorico P. Post-fire resource redistribution and fertility island dynamics in shrub encroached desert grasslands: a modeling approach. Landsc Ecol (2009) 2009;24:325–35. http://dx.doi.org/10.1007/s10980-008-9307-7.
[80] Ravi S, Breshears DD, Huxman TE, D'Odorico P. Land degradation in drylands: interactions among hydrologic-aeolian processes and vegetation dynamics. Geomorphology 2010;116:236–45.
[81] Reynolds JF, Virginia RA, Kemp PR, de Soyza AG, Tremmel DC. Impact of drought on desert shrubs: effects of seasonality and degree of resource island development. Ecol Monogr 1999;69:69–106.
[82] Rizvi SJH, Rizvi V. Allelopathy: Basic and applied aspects, 480. London: Chapman & Hall; 1992.
[83] Runyan CW, D'Odorico P, Lawrence D. Physical and biological feedbacks on deforestation. Rev Geophys 2012;50:RG4006. http://dx.doi.org/10.1029/2012RG000394.
[84] Scanlon TM, Caylor KK, Levin SA, Rodriguez-Iturbe I. Positive feedbacks promote power-law clustering of Kalahari vegetation. Nature 2007;449(7159):209–12.
[85] Schlesinger WH, Reynolds JF, Cunningham GL, Huenneke LF, Jarrell WM, Virginia RA, et al. Biological feedbacks in global desertification. Science 1990;247:1043–8.
[86] Scholes RJ, Archer SR. Tree–grass interactions in savannas. Annu Rev Ecol Syst 1997;28:517–44.
[87] Sitch S, Smith B, Prentice IC. Evaluation of ecosystem dynamics, plant geography and terrestrial carbon cycling in the LPJ dynamic global vegetation model. Glob Chang Biol 2003;9:161–85.
[88] Stewart J, Parsons AJ, Wainwright J, Okin GS, Bestelmeyer BT, Fredrickson EL, et al. Modeling emergent patterns of dynamic desert ecosystems. Ecol Monogr 2014;84:373–410.
[89] Tebaldi C, Mearns L, Nychka D, Smith R. Regional probabilities of precipitation change: a Bayesian analysis of multi-model simulations. Geophys Res Lett 2004;31:L24213. http://dx.doi.org/10.1029/2004GL021276.
[90] Turnbull L, Wainwright J, Brazier RE. Changes in hydrology and erosion over a transition from grassland to shrubland. Hydrol Process 2010;24:393–414.
[91] Turnbull L, Wainwright J, Brazier RE. Hydrological and erosion responses to vegetation change: a transition from semi-arid grassland to shrubland. Hydrol Process 2010;24:393–414.
[92] van Auken OW. Shrub invasions of North American semiarid grasslands. Annu Rev Ecol Syst 2000;31:197–215.
[93] van Auken OW. Causes and consequences of woody plant encroachment into western North American grasslands. J Environ Manag 2009;90:2931–42.
[94] van Wijk MT, Rodriguez-Iturbe I. Tree-grass competition in space and time: insights from a simple cellular automata model based on ecohydrological dynamics. Water Resour Res 2002;38 18-1–18-15.
[95] Whicker JJ, Breshears DD, Wasiolek PT, Kirchner TB, Tavani RA, Schoep DA, et al. Temporal and spatial variation of episodic wind erosion in unburned and burned semiarid shrubland. J Environ Qual 2002;31:599–612.
[96] White CS, Pendleton RL, Pendleton BK. Response of two semiarid grasslands to a second fire application. Rangel Ecol Manag 2006;59:98–106.
[97] Yu K, D'Odorico P. An ecohydrological framework for grass displacement by woody plants in savannas. J Geophys Res Biogeosci 2014;119:192–206. http://dx.doi.org/10.1002/2013JG002577.
[98] Zhou X, Istanbulluoglu E, Vivoni ER. Modeling the ecohydrological role of aspect-controlled radiation on tree-grass-shrub coexistance in a semiarid climate. Water Resour Res 2013;49(5):2872–95.